Michigan Technological University

Digital Commons @ Michigan Tech

Department of Geological and Mining Engineering and Sciences Publications

Department of Geological and Mining Engineering and Sciences

4-3-2004

Re-evaluation of SO2 release of the 15 June 1991 Pinatubo eruption using ultraviolet and infrared satellite sensors

Song Guo
Michigan Technological University

Gregg J. S. Bluth
Michigan Technological University

William I. Rose
Michigan Technological University

M. I. Watson
Michigan Technological University

A. J. Prata
CSIRO Atmospheric Research

Follow this and additional works at: https://digitalcommons.mtu.edu/geo-fp

 Part of the Geology Commons, Mining Engineering Commons, and the Other Engineering Commons

Recommended Citation

Guo, S., Bluth, G. J., Rose, W. I., Watson, M. I., & Prata, A. J. (2004). Re-evaluation of SO2 release of the 15 June 1991 Pinatubo eruption using ultraviolet and infrared satellite sensors. *AGU Publications, 5*(4). http://dx.doi.org/10.1029/2003GC000654
Retrieved from: https://digitalcommons.mtu.edu/geo-fp/47

Follow this and additional works at: https://digitalcommons.mtu.edu/geo-fp

 Part of the Geology Commons, Mining Engineering Commons, and the Other Engineering Commons

Geochemistry Geophysics Geosystems G3
AN ELECTRONIC JOURNAL OF THE EARTH SCIENCES
Published by AGU and the Geochemical Society

Article
Volume 5, Number 4
3 April 2004
Q04001, doi:10.1029/2003GC000654
ISSN: 1525-2027

Re-evaluation of SO_2 release of the 15 June 1991 Pinatubo eruption using ultraviolet and infrared satellite sensors

Song Guo
Department of Geological Engineering and Sciences, Michigan Technological University, Houghton, Michigan 49931, USA

Now at Department of Atmospheric and Oceanic Sciences, McGill University, 805 Sherbrooke Street West, Montreal, Quebec H3A 2K6, Canada (songguo@zephyr.meteo.mcgill.ca)

Gregg J. S. Bluth, William I. Rose, and I. Matthew Watson
Department of Geological Engineering and Sciences, Michigan Technological University, Houghton, Michigan 49931, USA

A. J. Prata
CSIRO Atmospheric Research, PB 1 Aspendale, Victoria, Australia

[1] In this study, ultraviolet TOMS (Total Ozone Mapping Spectrometer) satellite data for SO_2 are re-evaluated for the first 15 days following the 15 June 1991 Pinatubo eruption to reflect new data retrieval and reduction methods. Infrared satellite SO_2 data from the TOVS/HIRS/2 (TIROS (Television Infrared Observation Satellite) Optical Vertical Sounder/High Resolution Infrared Radiation Sounder/2) sensor, whose data sets have a higher temporal resolution, are also analyzed for the first time for Pinatubo. Extrapolation of SO_2 masses calculated from TOMS and TOVS satellite measurements 19–118 hours after the eruption suggest initial SO_2 releases of 15 ± 3 Mt for TOMS and 19 ± 4 Mt for TOVS, including SO_2 sequestered by ice in the early Pinatubo cloud. TOVS estimates are higher in part because of the effects of early formed sulfate. The TOMS SO_2 method is not sensitive to sulfate, but can be corrected for the existence of this additional emitted sulfur. The mass of early formed sulfate in the Pinatubo cloud can be estimated with infrared remote sensing at about 4 Mt, equivalent to 3 Mt SO_2. Thus the total S release by Pinatubo, calculated as SO_2, is 18 ± 4 Mt based on TOMS and 19 ± 4 Mt based on TOVS. The SO_2 removal from the volcanic cloud during 19–374 hours of atmospheric residence describes overall e-folding times of 25 ± 5 days for TOMS and 23 ± 5 days for TOVS. These removal rates are faster in the first 118 hours after eruption when ice and ash catalyze the reaction, and then slow after heavy ash and ice fallout. SO_2 mass increases in the volcanic cloud are observed by both TOMS and TOVS during the first 70 hours after eruption, most probably caused by the gas-phase SO_2 release from sublimating stratospheric ice-ash-gas mixtures. This result suggests that ice-sequestered SO_2 exists in all tropical volcanic clouds, and at least partially explains SO_2 mass increases observed in other volcanic clouds in the first day or two after eruption.

Components: 10,614 words, 7 figures, 5 tables, 2 videos.

Keywords: Satellite remote sensing; Pinatubo eruption; SO_2 release; volcanic eruptions.

Index Terms: 0370 Atmospheric Composition and Structure: Volcanic effects (8409); 1640 Global Change: Remote sensing; 0320 Atmospheric Composition and Structure: Cloud physics and chemistry.

Received 25 October 2003; **Revised** 6 January 2004; **Accepted** 20 January 2004; **Published** 3 April 2004.

Copyright 2004 by the American Geophysical Union

Guo, S., G. J. S. Bluth, W. I. Rose, I. M. Watson, and A. J. Prata (2004), Re-evaluation of SO_2 release of the 15 June 1991 Pinatubo eruption using ultraviolet and infrared satellite sensors, *Geochem. Geophys. Geosyst.*, *5*, Q04001, doi:10.1029/2003GC000654.

1. Introduction

[2] Mount Pinatubo is located at 15°08′N, 120°21′E in western Luzon, Philippines. After weeks of precursory activity, the largest eruption of the past 25 years occurred around 13:42 (local time) on 15 June 1991 and lasted for more than 9 hours [*Wolfe and Hoblitt*, 1996]. In this paper we examine ultraviolet and infrared satellite data for 15 days following the eruption.

[3] Satellite-based studies of volcanic gases have largely relied on ultraviolet sensing of sulfur dioxide. *Krueger* [1983] used the Total Ozone Mapping Spectrometer (TOMS) on NASA's Nimbus-7 satellite to map the volcanic SO_2 cloud from the 1982 El Chichón eruption. Since then, TOMS has been routinely used to trace the development and movement of volcanic clouds, and quantify volcanic SO_2 releases [*Krueger*, 1983; *Bluth et al.*, 1993; *Krueger et al.*, 1995, 2000; *Carn et al.*, 2003].

[4] The SO_2 volcanic clouds from the 1991 Mt. Pinatubo eruption were first studied using TOMS by *Bluth et al.* [1992]. Results include: (1) Total SO_2 mass released was estimated to be 20 Mt with an uncertainty of 30%; (2) An SO_2 removal/conversion rate (e-folding time) was estimated to be 35 days; and (3) The SO_2 cloud, moving westerly, encircled the Earth in about 22 days.

[5] The SO_2 budget for the 1991 Pinatubo eruption was also studied using the Nimbus-7 Solar Backscatter Ultraviolet Spectrometer (SBUV/2) data from 1 July and 17 July by *McPeters* [1993], who concluded: (1) An estimated total SO_2 mass release of 12–15 Mt (the accuracy was reported as 10–20%, but *Schnetzler et al.* [1995] pointed out that this referred to individual measurements, and that the uncertainty in the SBUV-derived cloud mass estimate, based on only two data points, must be significantly higher.) (2) An estimate of SO_2 e-folding time of 24 days.

[6] *Reed et al.* [1993] used data 100–170 days after the eruption from the Microwave Limb Sounder (MLS) experiment on the Upper Atmosphere Research Satellite (UARS) to infer that the initially erupted SO_2 mass was 17 Mt and the SO_2 e-folding time was 33 days (no uncertainties were estimated).

[7] This paper is a re-evaluation of the Pinatubo SO_2 emission using TOMS, and includes new analyses using infrared satellite data. This new study is important because: (1) Pinatubo was the largest and most atmospherically significant event of the satellite era and the data have been widely cited and used with climate models [e.g., *Bekki and Pyle*, 1994; *Timmreck et al.*, 1999; *Liu and Penner*, 2002; *Robock*, 2002]. (2) TOMS data have been reprocessed for an improved accuracy [*McPeters et al.*, 1996]. (3) A new TOMS algorithm has been developed for providing more accurate SO_2 results [*Krueger et al.*, 2000]. (4) Analytical techniques are available to help resolve problems of missing data and incomplete or redundant coverage from orbital and swath characteristics (this paper). (5) A new infrared SO_2 retrieval algorithm, using measurements from the High-resolution Infrared Radiation Sounder/2 (HIRS/2) on NOAA's TIROS Operational Vertical Sounder (TOVS) platform, has been demonstrated by A. J. Prata, W. I. Rose, S. Self, and D. M. O'Brien (Global, long-term sulphur dioxide measurements from TOVS data: A new tool for studying explosive volcanism and climate, manuscript submitted to *Journal of Geophysical Research*, 2004, hereinafter referred to as Prata et al., submitted manuscript, 2004) (TOVS/HIRS/2 sensor is referred as TOVS sensor in this paper). The use of TOVS data provides higher spatial (17.5 km versus 50 km at nadir) and temporal resolution volcanic SO_2 cloud images (several times a day compared to once per day

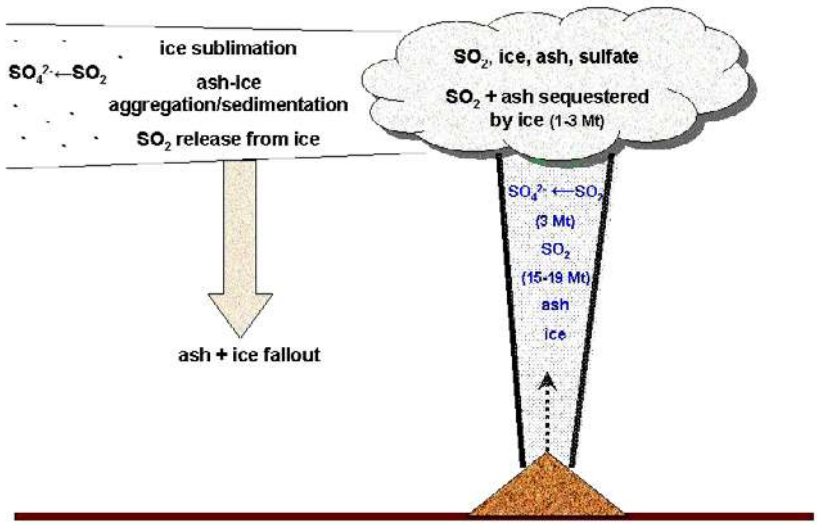

Figure 1. Schematic figure showing how ice, ash, sulfate are distributed in Pinatubo's rising plume and drifting volcanic cloud.

for TOMS). Together with TOMS SO_2 cloud images, a better understanding of the development of the Pinatubo volcanic SO_2 cloud and a better estimate of the fate of SO_2 within the volcanic cloud is achieved.

[8] Huge masses of volcanic ash and gas, mixed with hydrometeors, were directly emitted into the stratosphere by Pinatubo and this resulted in global environmental, atmospheric, and climatic effects for up to several years. The most significant atmospheric effects included: (1) Large stratospheric sulfate aerosol loading with chemical and dynamic perturbations affecting stratospheric NO_2, reactive chlorine, and ozone concentrations and increasing stratospheric opacity [*McCormick et al.*, 1995]; (2) Cooling effects in the troposphere (more solar radiation scattering back to space) and warming effects in the stratosphere (infrared absorptivity of stratospheric aerosols) [*McCormick et al.*, 1995]. Summer surface cooling (average $-3°C$) and winter surface warming (average $+3°C$) were found in the northern hemisphere 1–2 years after eruption [*Robock*, 2002]; (3) Destruction of stratospheric ozone after the eruption due to both heterogeneous reactions occurring on the surface of sulfate aerosol (similar to heterogeneous reactions that occur within polar stratospheric clouds responsible for the Antarctic Ozone Hole [*Solomon et al.*, 1993]), and circulation changes after the eruption [*Kinne et al.*, 1992]; and (4) Climatic effects worldwide which lasted for up to several years after eruption [*Robock*, 2002]. Because Pinatubo was the largest and most climatically significant eruption in recent years it is important that the stratospheric loading be illuminated so that we can learn how to scale the atmospheric effects of eruptions (Figure 1). There are also important volcanological questions concerning the nature of the eruption that may be tested by the data we report on the volcanic cloud, such as the importance of co-ignimbrite cloud processes [*Dartevelle et al.*, 2002] and the excess of sulfur in the eruption [*Gerlach et al.*, 1996; *Wallace et al.*, 2003].

2. Methods Used for SO_2 Retrieval

[9] The characteristics of the TOMS and TOVS satellite sensors are summarized in Table 1. One daily TOMS SO_2 measurement around local solar noon and 6 TOVS measurements each day for the first 15 days after eruption are available for this study (2 images from each NOAA-n satellite), though some days only 5 measurements are usable.

2.1. TOMS

[10] The Total Ozone Mapping Spectrometer (TOMS) was mainly designed and used to monitor

Table 1. Characteristics of TOMS and TOVS Satellite Sensors[a]

TOMS[b]			TOVS[c]		
Channel	Wavelength, μm	Application	Channel	Wavelength, μm	Application
1	312.3	SO_2	5	13.97	sulfate
2	317.3	SO_2	6	13.64	sulfate
3	331.1	SO_2, AI	7	13.35	sulfate
4	339.7	SO_2	8	11.11	sulfate
5	359.9	SO_2, AI	9	9.71	sulfate
6	380.0		10	8.16	sulfate
			11	7.33	SO_2[d]

[a] AI (Aerosol Index), which is the difference of the measured spectral contrast between the 331.1 nm and 359.9 nm radiances and the spectral contrast between the 331.1 nm and 359.9 nm radiances, is an index representing the ash and aerosol within the volcanic cloud qualitatively [*Seftor et al.*, 1997; *Krotkov et al.*, 1999].
[b] *McPeters et al.* [1996]. Spatial resolution is 50 km (nadir).
[c] *Yu and Rose* [2000]. Spatial resolution is 17.5 km (nadir).
[d] *Prata et al.* [2004].

the total column amount of ozone (O_3) globally. However, because SO_2 absorbs similarly to O_3 in the wavelengths used by TOMS, *Krueger et al.* [1983] developed a method to discriminate, and quantify, SO_2. Since then, TOMS has been routinely used to trace the development and movement of volcanic clouds, quantify volcanic SO_2 amounts, and obtain information on ash particles in volcanic clouds [*Krueger et al.*, 1983; *Bluth et al.*, 1993; *Krueger et al.*, 1995, 2000]. The TOMS wavelengths used for SO_2 retrieval are summarized in Table 1.

[11] The TOMS Matrix Inversion algorithm [*Krueger et al.*, 1995] was used in the initial estimate of Pinatubo's SO_2 emission by *Bluth et al.* [1992]. This method uses a linear model of scattering and absorption and a matrix inversion technique to simultaneously determine the total column amounts of ozone and sulfur dioxide. Here we use an updated algorithm ("Iterative" algorithm) described in *Krueger et al.* [2000]. The Iterative algorithm is based on the Matrix Inversion algorithm except an effective optical path determined from a radiative transfer model is used instead of a geometric optical path. The Matrix Inversion uncertainty is estimated at ±10% for most central scan angles, and ±30% at large solar zenith angles near the swath edges [*Krueger et al.*, 1995]. We use Krueger et al.'s ±10% uncertainty because the Matrix Inversion and Iterative algorithms have basically the same considerations, and because the large (multiorbit) geographic areas covered by the Pinatubo gas cloud ensures that central scan angles will dominate. At moderate optical depths (0.3), volcanic ash and sulfate aerosol in the volcanic plume produced a 15–25% overestimation of sulfur dioxide for the Matrix Inversion algorithm [*Krueger et al.*, 1995]. In this paper the possibility of overestimation of SO_2 in early ash-rich and ice-rich Pinatubo volcanic clouds was reduced, because the emitted mass estimate was generated from 15 days of observations; thus, most of the sulfur dioxide mass data were unbiased by ash and ice interferences.

[12] TOMS SO_2 results have also been validated by ground measurement of SO_2 using a Brewer Spectrophotometer (Mount Spurr plume passing over Toronto on 19 September 1992) [*Krueger et al.*, 1995] and a correlation spectrometer (COSPEC) (Galunggung cloud in Indonesia from 19 August to 19 September 1982) [*Bluth et al.*, 1994]. The differences between Matrix Inversion algorithm and ground measurements were estimated to be less than 20–30% [*Krueger et al.*, 1995, 2000]. Because of the scanning and zenith angles of the volcanic cloud at the time of the Brewer measurements, errors of up to 30% were calculated for the Spurr case (owing to it's relatively small geographic cloud area) but the average geometry during TOMS Pinatubo cloud measurements is much more favorable.

2.2. TOVS

[13] SO_2 retrieval with TOVS is based on the antisymmetric stretch of the SO_2 molecule centered at

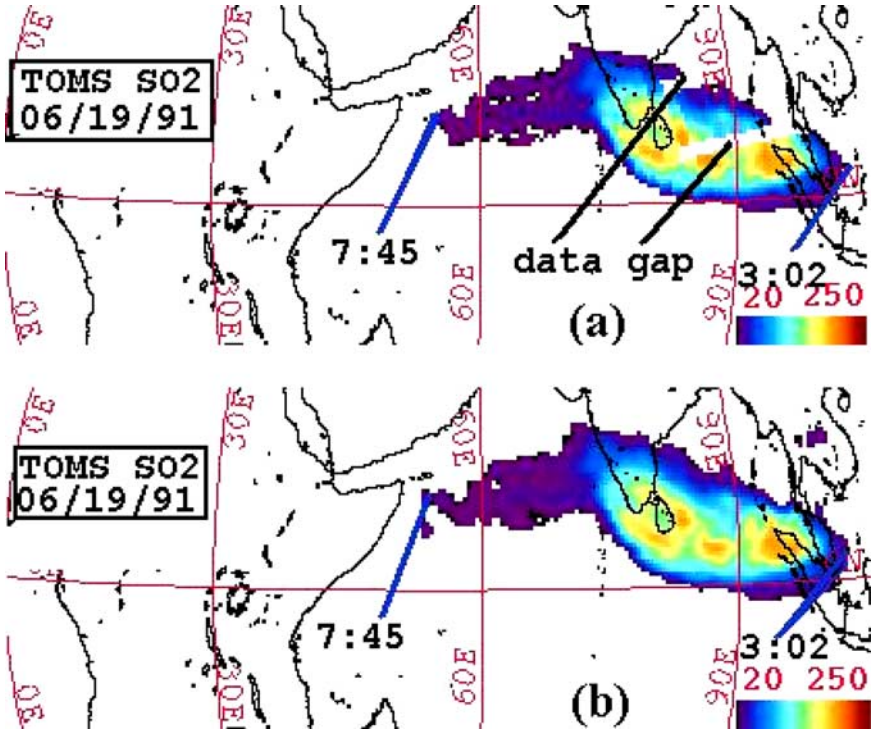

Figure 2. (a) TOMS SO_2 image with two data gaps sampled in Terascan™ (an image displaying software). (b) Reconstructed TOMS SO_2 image through Kriging method, showing reconstructed data. Latitude and longitude grid spacing is 30°. Linear bar scales have SO_2 values represented in Dobson Units (DU). The times (in GMT) represent the sensor observation times of the volcanic cloud. The solid blue lines point to an intersection of the orbital swath's central scan position with the volcanic cloud.

7.3 μm (Prata et al., submitted manuscript, 2004). The 7.3 μm channel of the TOVS instrument measures the absorption of both SO_2 and water vapor. The water vapor absorption for the 7.3 μm channel can be estimated by linearly interpolating the radiance of 6.7 μm and 11.1 μm channels. The difference between interpolated and measured radiance is assumed to be due to SO_2 absorption. Little silicate ash absorption exists in the 7.3 μm channel; therefore, no silicate ash effect needs to be considered in the calculation of SO_2 (Prata et al., submitted manuscript, 2004). The TOVS SO_2 retrieval algorithm is based on the radiative transfer model by *Pierluissi and Tomiyama* [1980]. The parameters that are critical to determine the retrieved SO_2 amount and total SO_2 mass within the whole volcanic cloud are: (1) an estimated SO_2 cloud height; (2) the atmospheric temperature profile; (3) the background "cutoff" value. The errors of the TOVS SO_2 retrieval are estimated to be 5–10% by Prata et al. (submitted manuscript, 2004).

[14] The maximum plume altitude of the main 1991 Pinatubo eruption is estimated to be ~39 km [*Holasek et al.*, 1996]. The neutral buoyant regions of the volcanic SO_2 and ash cloud are estimated to be 25 km and 22 km, respectively, using cloud positions derived from satellite sensors (TOMS, TOVS, AVHRR) and NASA isentropic wind trajectory model [*Guo et al.*, 2004]. *Reed et al.* [1993] also estimated that the SO_2 peak layer was around 26 km. The Pinatubo volcanic clouds are assumed to mainly travel in the neutral buoyant region several hours after the eruption stops. The estimated ranges of the neutral buoyant regions are consistent with other measurements: 17–26 km (lidar) by *DeFoor et al.* [1992], 20–23 km (balloon) by *Deshler et al.* [1992], 17–28 km (lidar) by *Jaeger* [1992], and 17–25 km (lidar) by *Avdyushin et al.* [1993]. In this study, an altitude of 25 km is used for all TOVS SO_2 retrievals. If the TOVS altitudes were assumed to be lower, for example

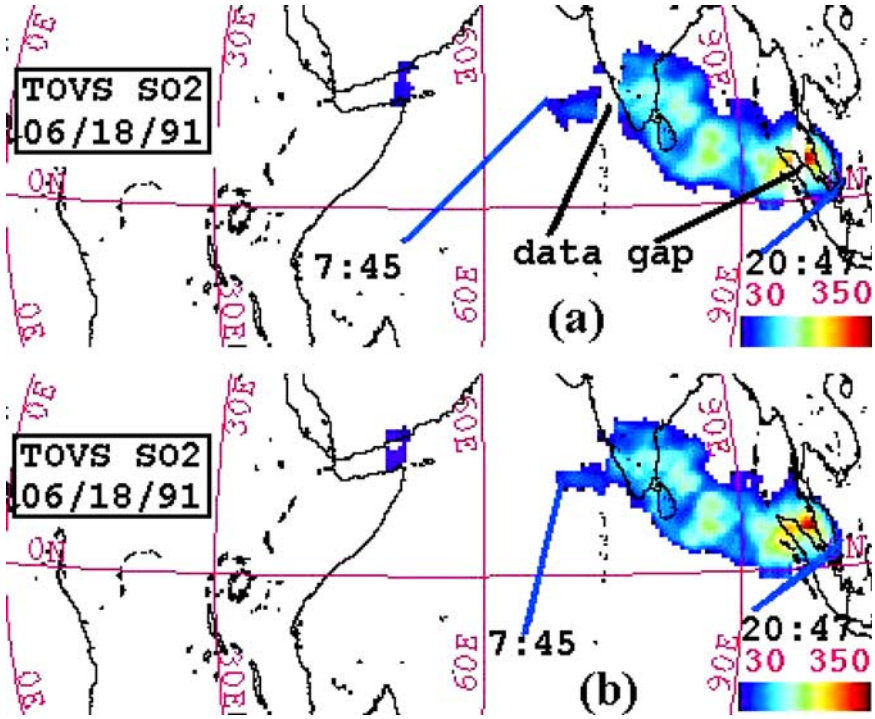

Figure 3. (a) TOVS SO_2 images with two orbit data gaps sampled in Terascan. (b) Reconstructed TOVS SO_2 image through nearest neighbor method, showing reconstructed orbit data. Latitude and longitude grid spacing is 30°. Linear bar scales have SO_2 values represented in Dobson Units (DU). The times (in GMT) represent the sensor observation times of the volcanic cloud. The solid blue lines point to an intersection of the orbital swath's central scan position with the volcanic cloud.

at 23 km, the SO_2 burdens would change by about 2–5%.

2.3. Enhancing Incomplete Satellite Coverage of Volcanic Cloud Masses

[15] Both systematic and random data gaps exist in the TOMS and TOVS data sets (Figures 2a and 3a). Past studies [e.g., *Bluth et al.*, 1992] have not attempted to correct for these chronic losses, and here we employ some image processing methods to produce contiguous two-dimensional (2-D) maps of volcanic SO_2 clouds which bridge data gaps.

[16] Although designed as a mapper, the curvature of the Earth as well as the TOMS sensor scanning produce small areas (up to 20% of the pixel area) in each scan line where the adjacent pixels overlap, as well as small areas which are not covered [*McPeters et al.*, 1996]. Random data gaps also occur, due to both sensor malfunctions and data losses during recording and transmission. In these cases, the typical losses consist of sequences of several missing scan lines (the missing part typically comprises 2°–3° in latitude and 24°–26° in longitude). For Pinatubo, random data gaps occur in almost every image, and often within the volcanic SO_2 cloud region (approximately 10% of the data are missing from the SO_2 cloud in days 2, 4, 5, and 7 after eruption).

[17] In the TOVS data set, systematic gaps occur owing to frequent calibration (3 scan lines after every 40, or every 256 seconds). Also, one or more large (2°–5° in longitude and within the whole latitude range) gaps exist between neighboring orbits, in all volcanic cloud images used in this study. Slight gaps also exist between scan lines. Overall for the TOVS Pinatubo data set, 10–30% of the data are missing in every image studied.

[18] Two methods of satellite image reconstruction are applied in this paper, which resample irregular satellite data to a regular grid. The TOMS data sets are resampled using a Punctual Kriging statistical analysis. However, owing to the relatively large gaps in the TOVS data sets [*Kidwell*, 1998], these were resampled using a nearest-neighbor interpola-

tion. These two resampling schemes are standard features available in Interactive Data Analysis (IDL)™ (http://www.rsinc.com/idl) software package we used to process and analyze the TOMS and TOVS data. In Figures 2a and 3a, TOMS and TOVS images are presented for 18 and 19 June 1991, respectively. These demonstrate both systematic (TOVS) and random (TOMS) gaps in coverage. Figures 2b and 3b show the reconstructed images using the above processing techniques.

[19] Visual inspection of the images suggests the reconstructions have not introduced any unreasonable values. In addition, each method was quantitatively tested by reconstructing gaps that were arbitrarily imposed (the imposed gap areas are the same as the actual gaps in the TOMS and TOVS data sets) in complete portions of TOMS and TOVS SO_2 cloud images. The Kriging method used for TOMS resulted in less than 2% error in total cloud mass; the nearest neighbor resampling for TOVS reproduced SO_2 masses to within 15% error. The larger error reflects the larger gaps in the data which occur in the TOVS data sets.

[20] If the edge of the volcanic cloud happens to be within the TOVS data gaps or data gaps occupy >30% of the whole cloud in area, the image reconstruction methods cannot provide a reliable total SO_2 tonnage. Therefore these images are not used in the estimation of initially erupted SO_2 or e-folding time in this paper. The image reconstruction method is also not applied to the TOVS SO_2 images for the first 19 hours after eruption as unmappable portions exist in the cloud due to the high opacity [*Guo et al.*, 2004].

3. Results

3.1. 2-D Mapping of Pinatubo Volcanic SO_2 Clouds

[21] TOMS and TOVS SO_2 maps are used to study the 2-D distribution of the volcanic SO_2 cloud (Figure 4, Animations 1 and 2; animations available in the HTML version of the article at http://www.g-cubed.org). The volcanic SO_2 cloud travels westerly along the same latitude, with slight dispersion to the south. It's leading edge from the 15 June main eruption (the high burden part of the cloud) reached the Indian mainland 3 days (06/18/91) after the eruption, and passed over Africa 5–10 days (06/20/91–06/25/91) after the eruption (Figure 4). The SO_2 clouds are well distinguished and easily identified from the background values for 15 days. The SO_2 cloud circled the earth about 21 days after the eruption. Note however, that the trailing edge of the cloud remained over the Indian Ocean and India. The detection and movement of the Pinatubo volcanic ash and aerosol masses, and their comparison with the SO_2 cloud, are detailed in *Guo et al.* [2004].

[22] The 2 dimensional volcanic cloud areas mapped by TOMS and TOVS increased from about $3–4 \times 10^6$ km^2 after 1 day to about 30×10^6 km^2 after 15 days (Figure 5a). The maximum SO_2 pixel value (column amount of SO_2) is about 530 Dobson Units (DU) 24 hours after eruption, ~100 DU one week after eruption, <50 DU two weeks after the eruption, and <10 DU three weeks after eruption, a value which is difficult to distinguish from the background pixel values (Figure 5a and Tables 2 and 3).

3.2. Comparison of the TOMS and TOVS Pinatubo Volcanic Cloud Images

[23] Sequential TOMS and TOVS images generally record similar SO_2 spatial patterns (Figure 4). This consistency can also be verified by the cloud burden (tonnage/area) data shown in Figure 5 and Tables 2 and 3. In the first 4–5 days, there appear to be two overlapping clouds: a weaker SO_2 cloud (pixel values <60 DU) to the west is likely due to precursory activity that started on 12 June 1991, while a region with higher burdens of SO_2 (max-

Figure 4. Sequence of TOMS and TOVS (NOAA-10, NOAA-11, NOAA-12) SO_2 cloud images for 15 days after eruption, showing the development and spatial pattern of the Pinatubo volcanic SO_2 cloud. The images are displayed in the order of sensing time (GMT). Latitude and longitude grid spacing is 30°. Linear bar scales have SO_2 values represented in Dobson Units (DU). The times (in GMT) represent the sensor observation times of the volcanic cloud. The solid blue lines point to an intersection of the orbital swath's central scan position with the volcanic cloud. Where no lines are used, the time represents the observation time of the cloud's centroid.

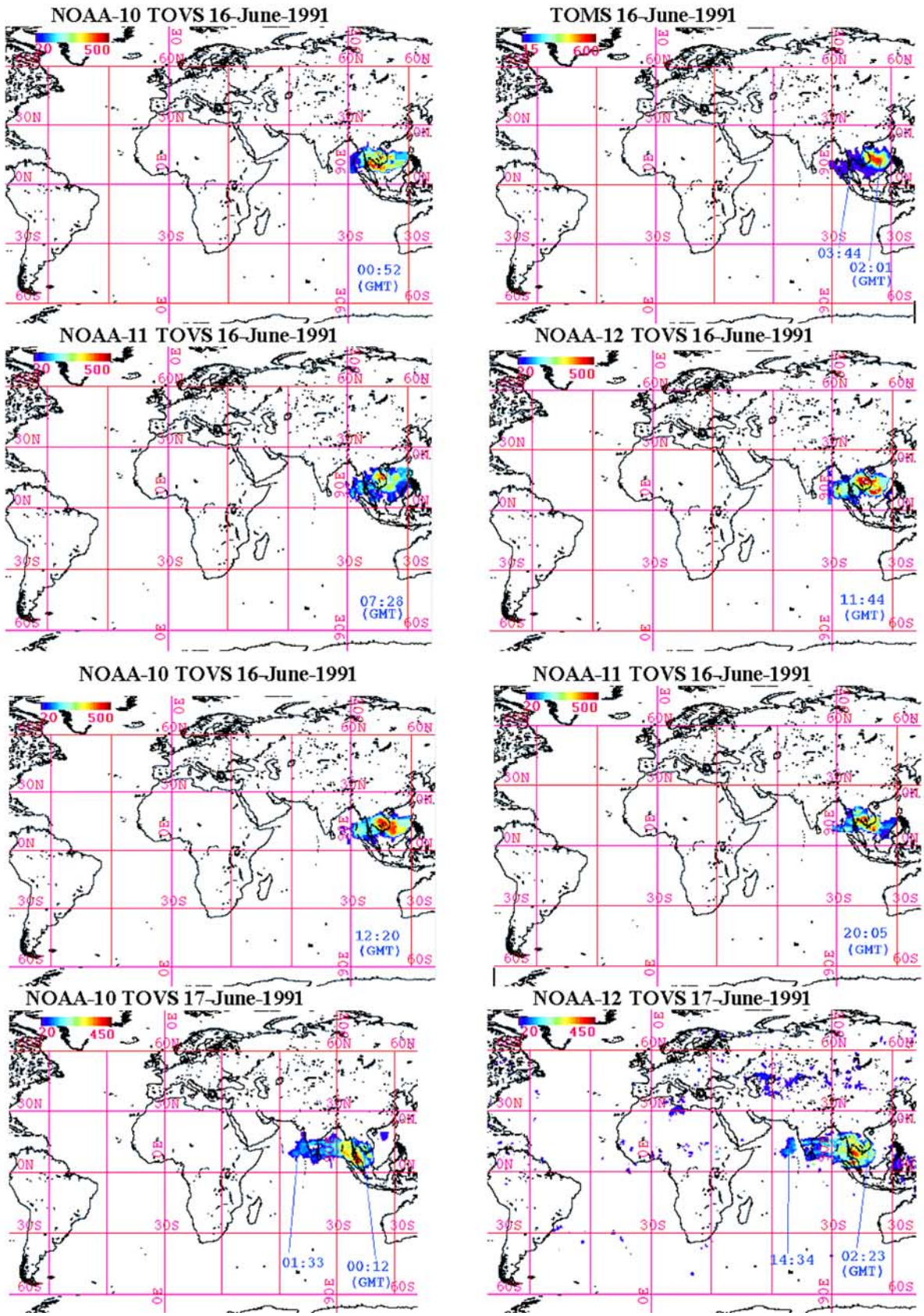
NOAA-10 TOVS 16-June-1991
00:52 (GMT)
TOMS 16-June-1991
03:44
02:01 (GMT)
NOAA-11 TOVS 16-June-1991
07:28 (GMT)
NOAA-12 TOVS 16-June-1991
11:44 (GMT)
NOAA-10 TOVS 16-June-1991
12:20 (GMT)
NOAA-11 TOVS 16-June-1991
20:05 (GMT)
NOAA-10 TOVS 17-June-1991
01:33
00:12 (GMT)
NOAA-12 TOVS 17-June-1991
14:34
02:23 (GMT)

Figure 4.

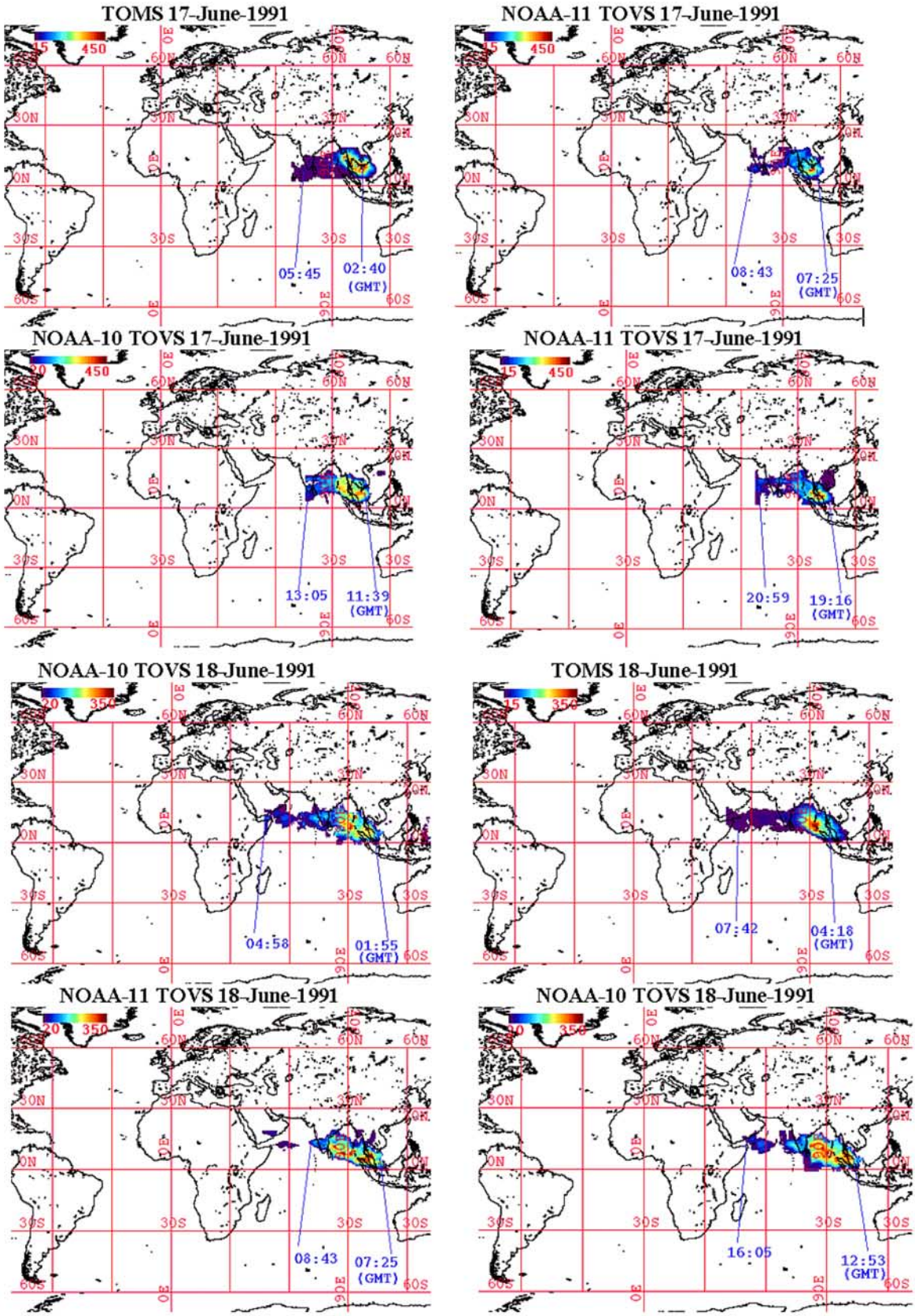

Figure 4. (continued)

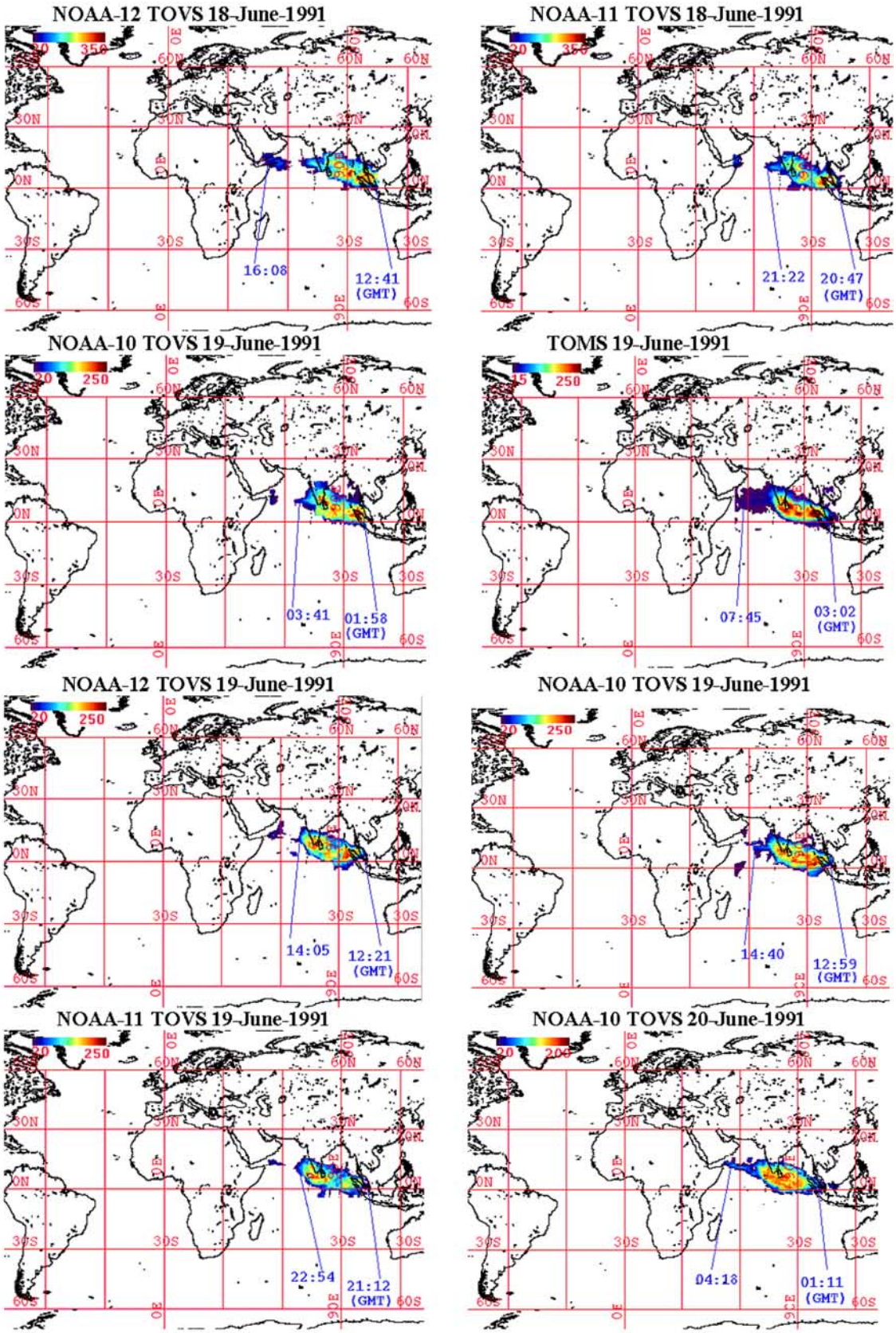

Figure 4. (continued)

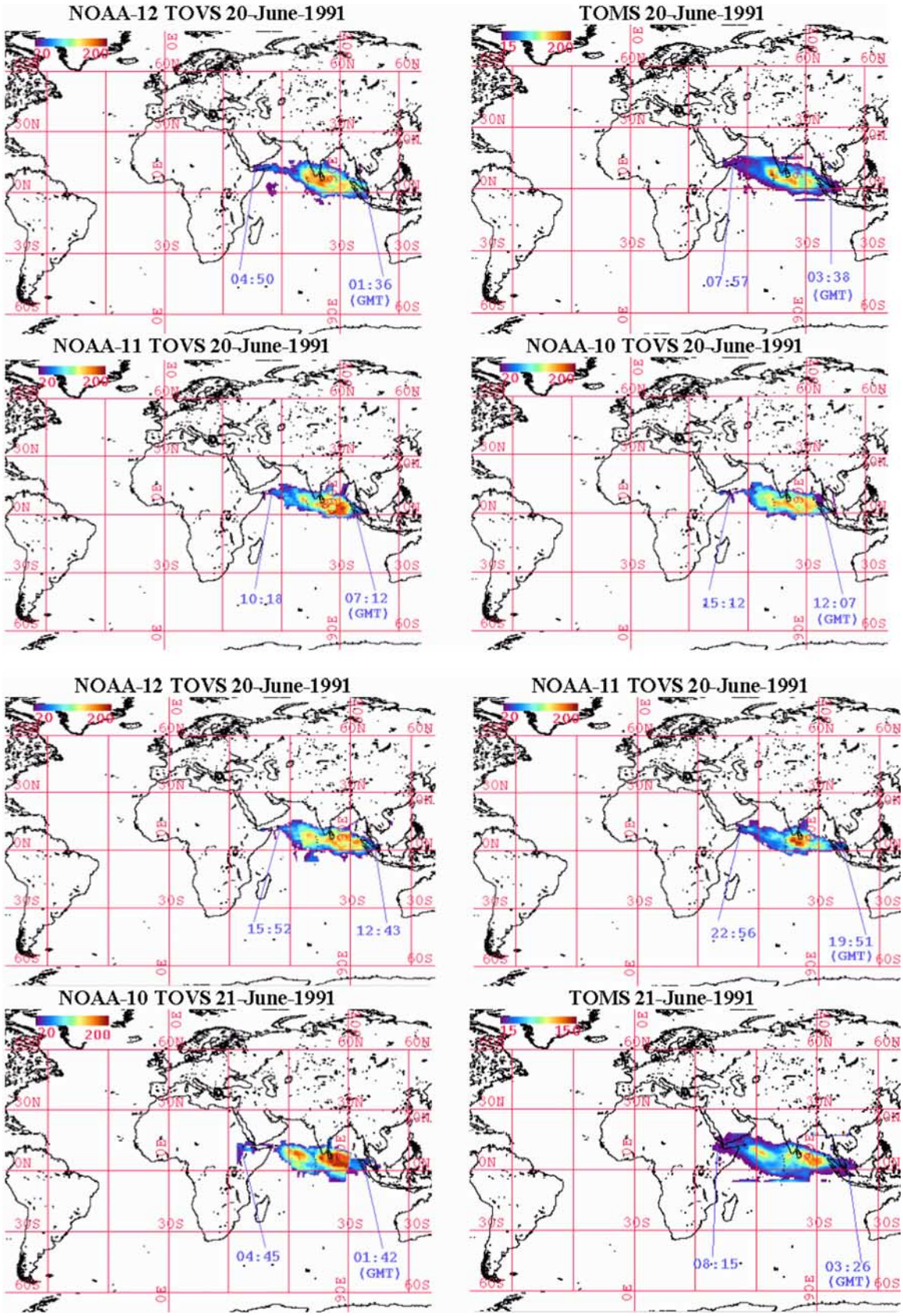

Figure 4. (continued)

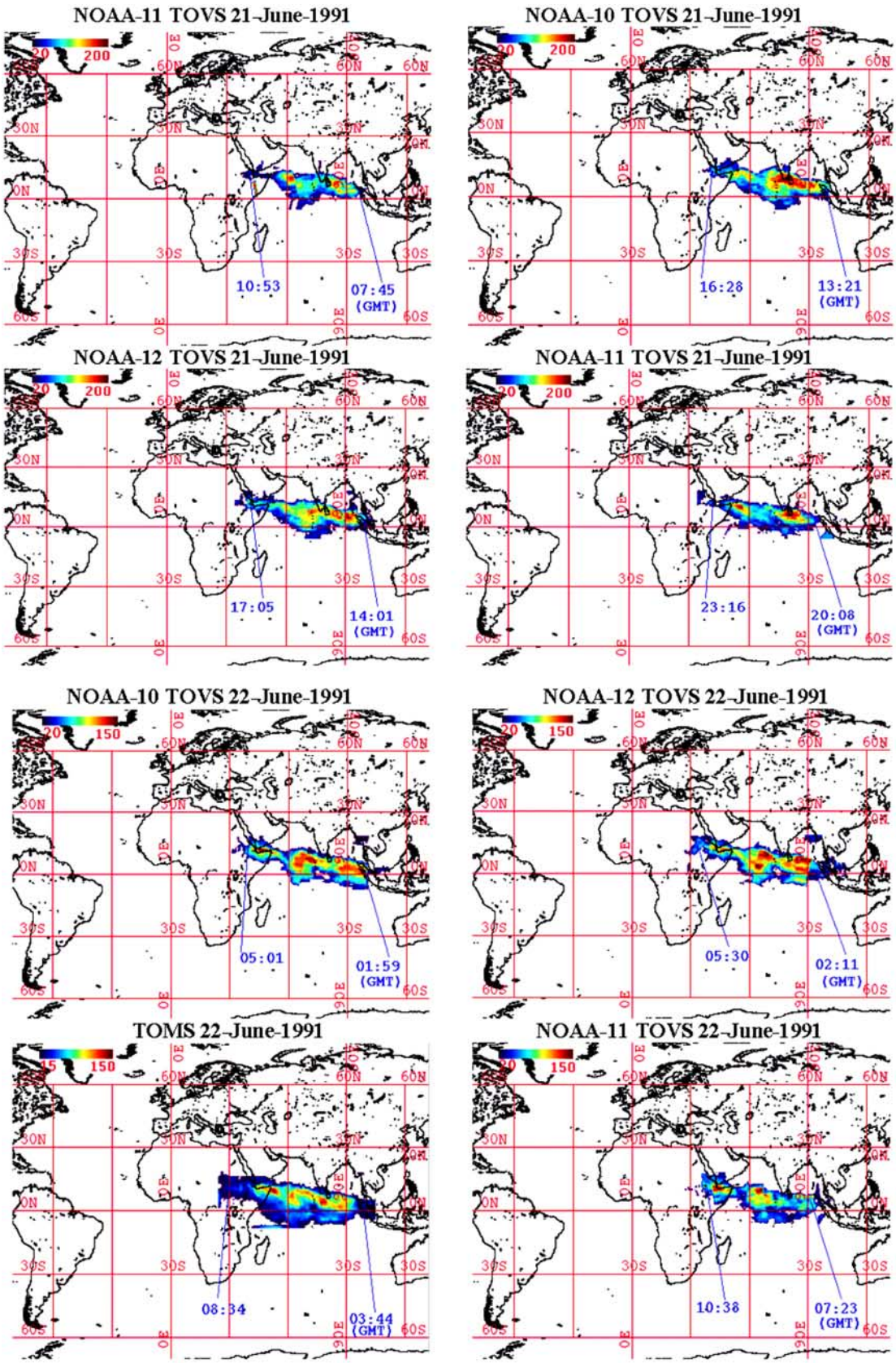

Figure 4. (continued)

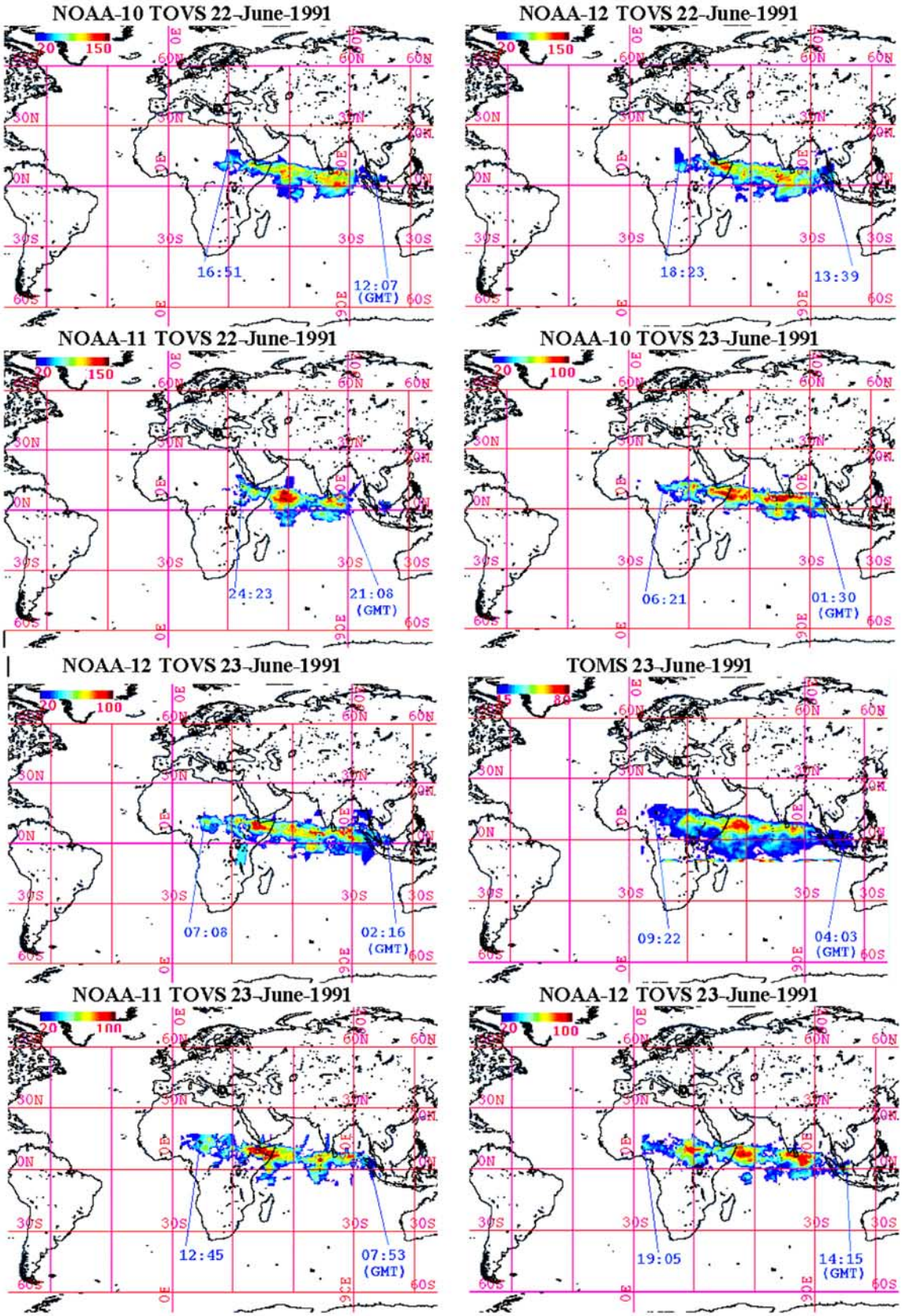

Figure 4. (continued)

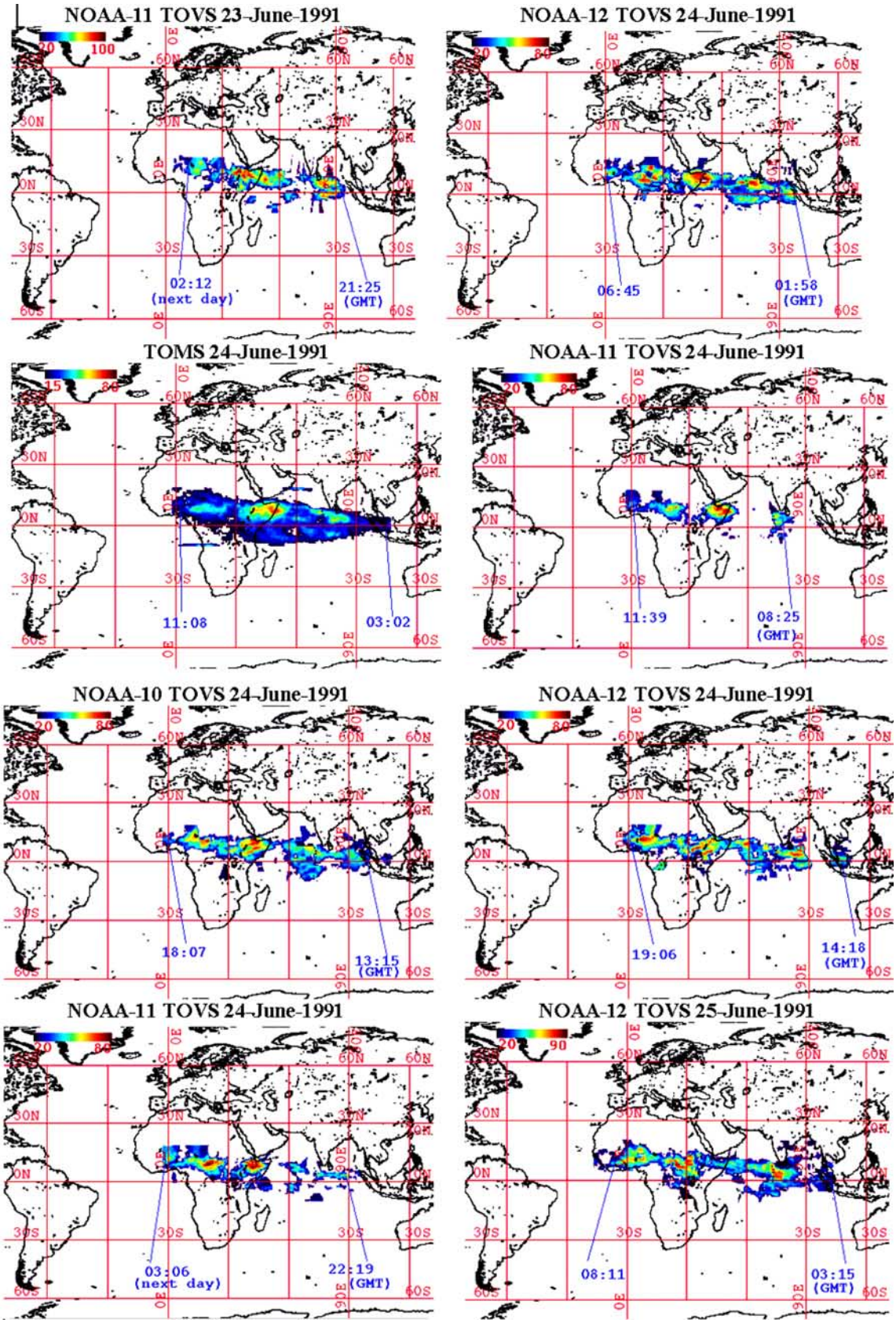

Figure 4. (continued)

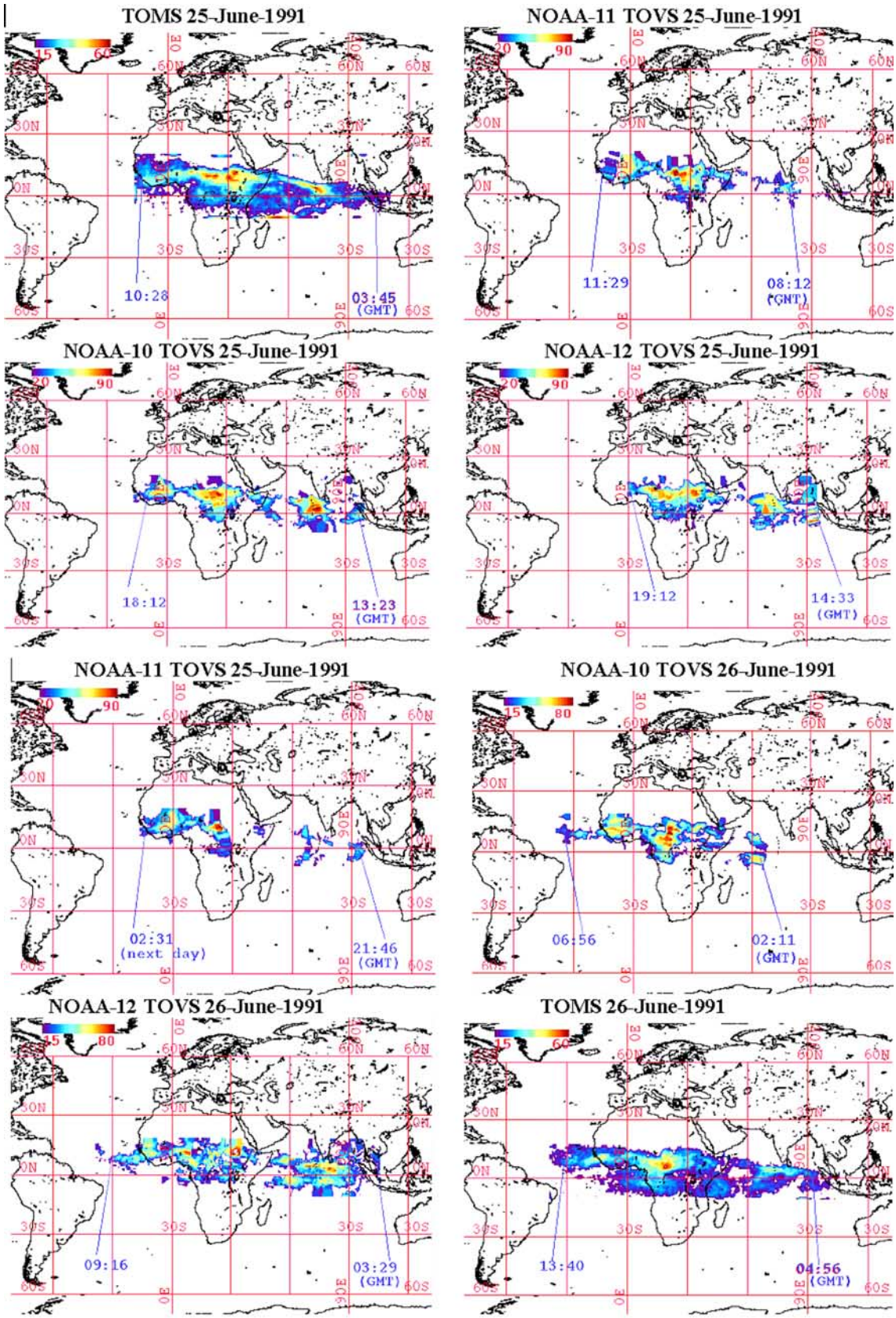

Figure 4. (continued)

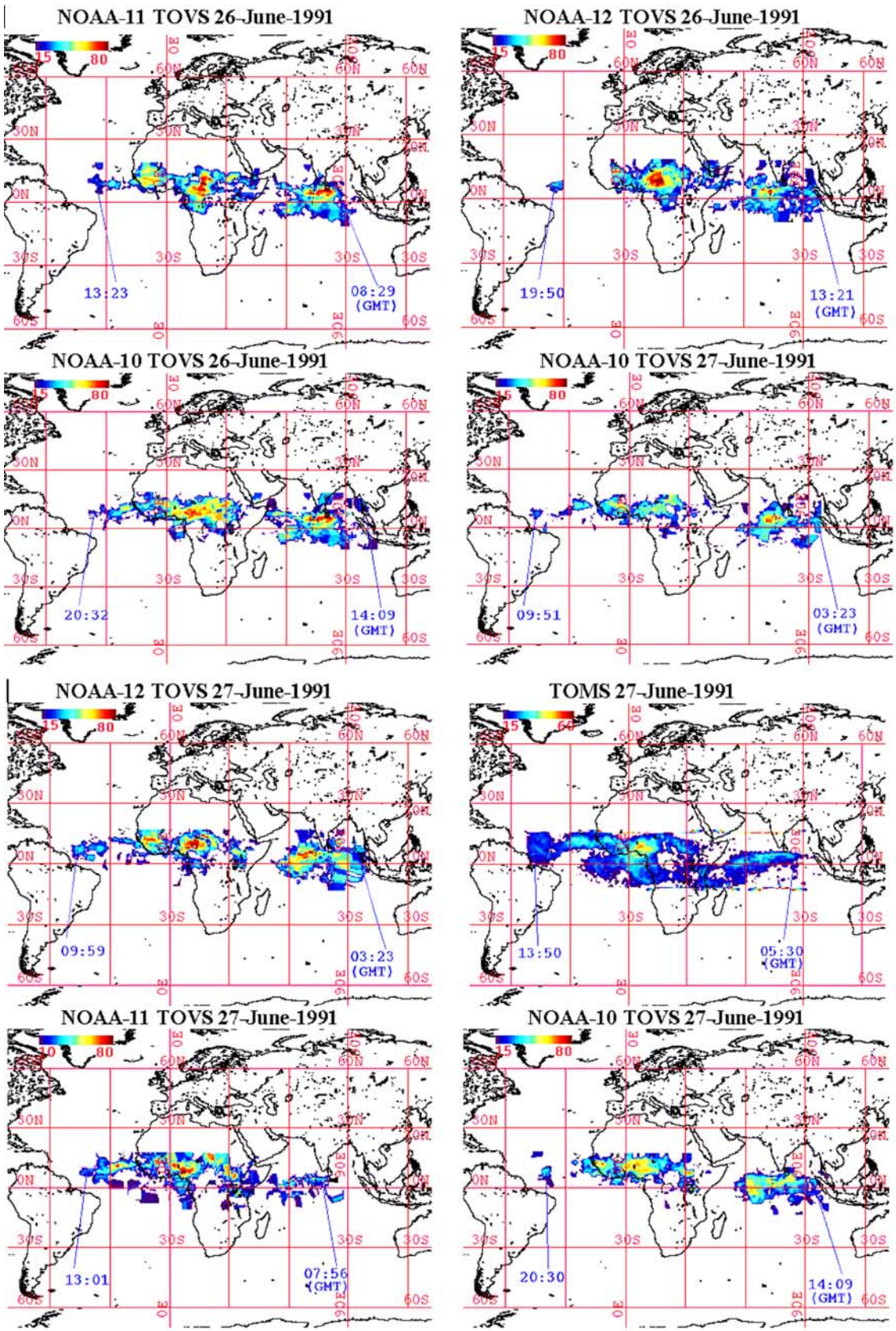

Figure 4. (continued)

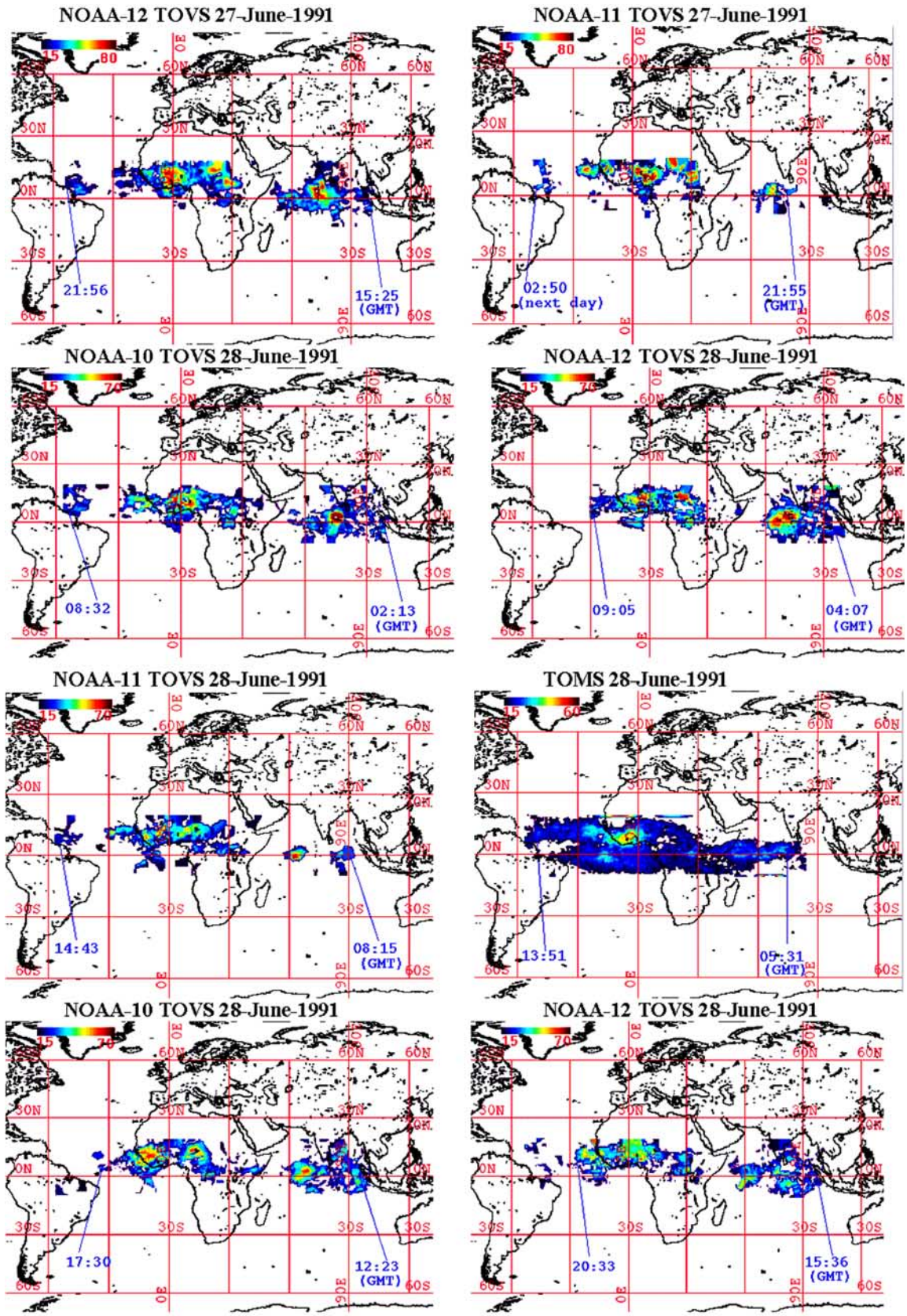

Figure 4. (continued)

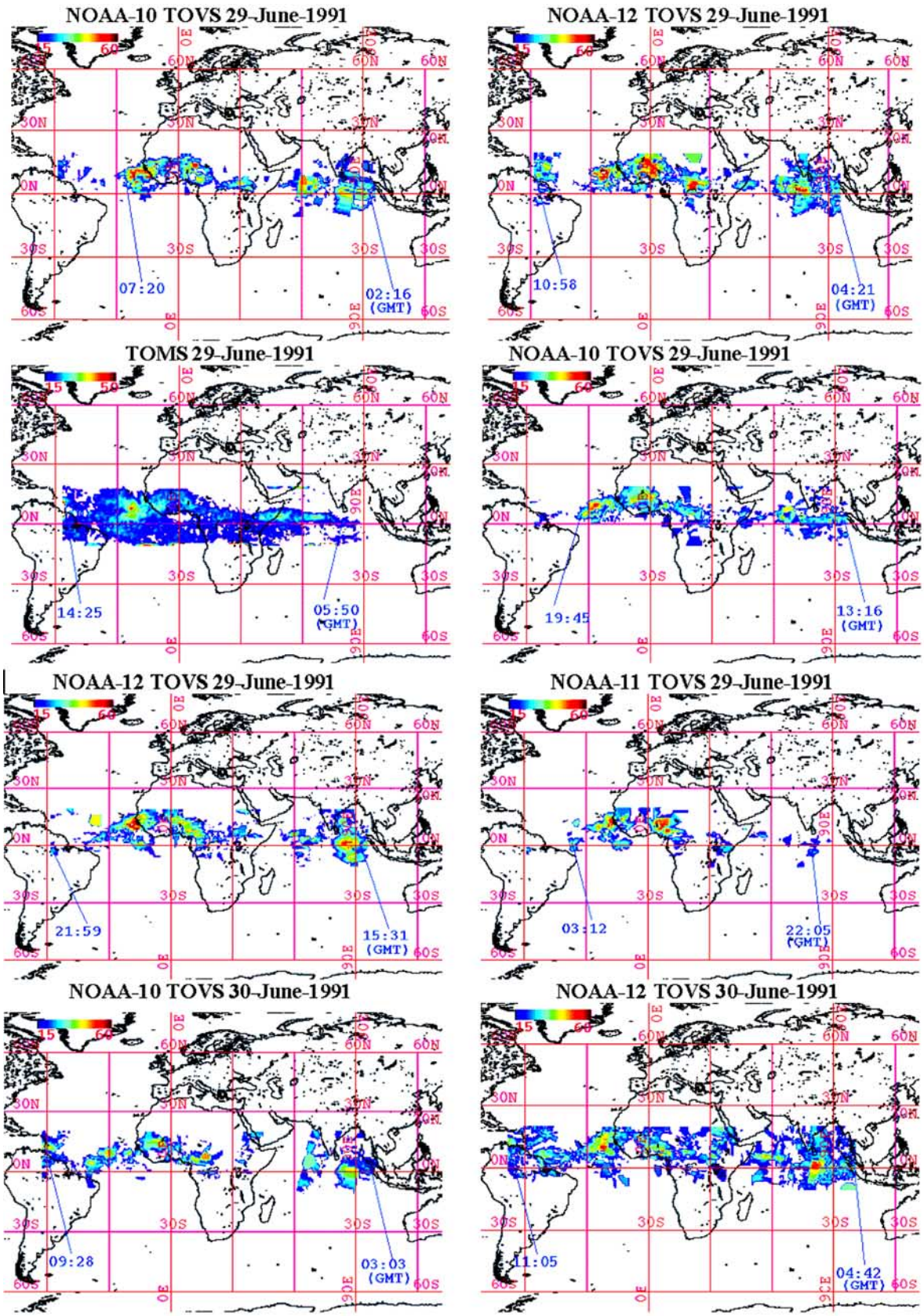

Figure 4. (continued)

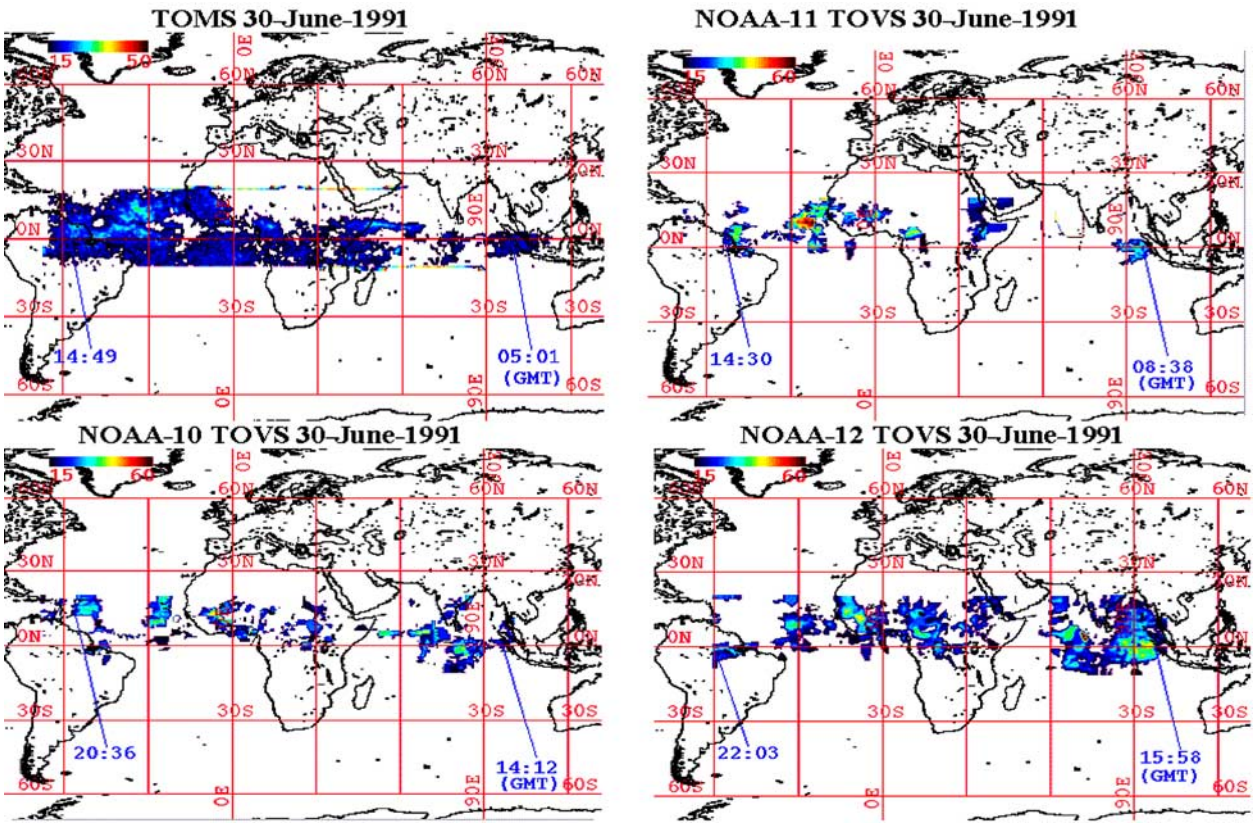

Figure 4. (continued)

imum pixel value >500 DU) to the east is from the main eruption. Both TOMS and TOVS sensors map the weaker cloud to the west for the first 3 days after eruption. On the fourth day (06/19/91), the lower burden areas to the west disappear in TOVS while still visible in the TOMS SO_2 map. TOMS cloud areas are generally larger than TOVS cloud areas, especially one week after eruption. The TOVS cloud is also not as contiguous as TOMS cloud one week after eruption. The reason for these discrepancies is probably water vapor interference of the TOVS sensor from the meteorological cloud below the SO_2 clouds. Prata et al. (submitted manuscript, 2004) point out that SO_2 will not be detected by TOVS if elevated water vapor occurs in the troposphere just below the SO_2 cloud, and the effect will be worse if the SO_2 cloud is thin (i.e., SO_2 values <30 DU). The high water vapor within the tropical troposphere affects the TOVS SO_2 detection, especially for the low value regions, making these regions undetectable. This means the higher water vapor below SO_2 cloud actually results in a higher detection limit for the TOVS SO_2 retrieval (Prata et al., submitted manuscript, 2004). Water vapor in the stratosphere is explicitly not considered here. It is likely that substantial stratospheric water vapor would lead to an overestimate of SO_2 by TOVS.

[24] TOVS SO_2 total cloud masses are 5–30% higher than TOMS values (Tables 2 and 3 and Figure 5a). The percent difference of maximum SO_2 pixel values from TOVS and TOMS ((TOVS-TOMS)/TOMS) increases over time and the maximum pixel values from TOVS get up to 40–50% higher than those from TOMS 370 hours after eruption (Figure 6). The opposing trends of cloud areas from the two sensors (Figure 5a) tend to balance the calculated cloud SO_2 masses, especially one week after eruption. The reasons for the higher TOVS values are likely due to effects of

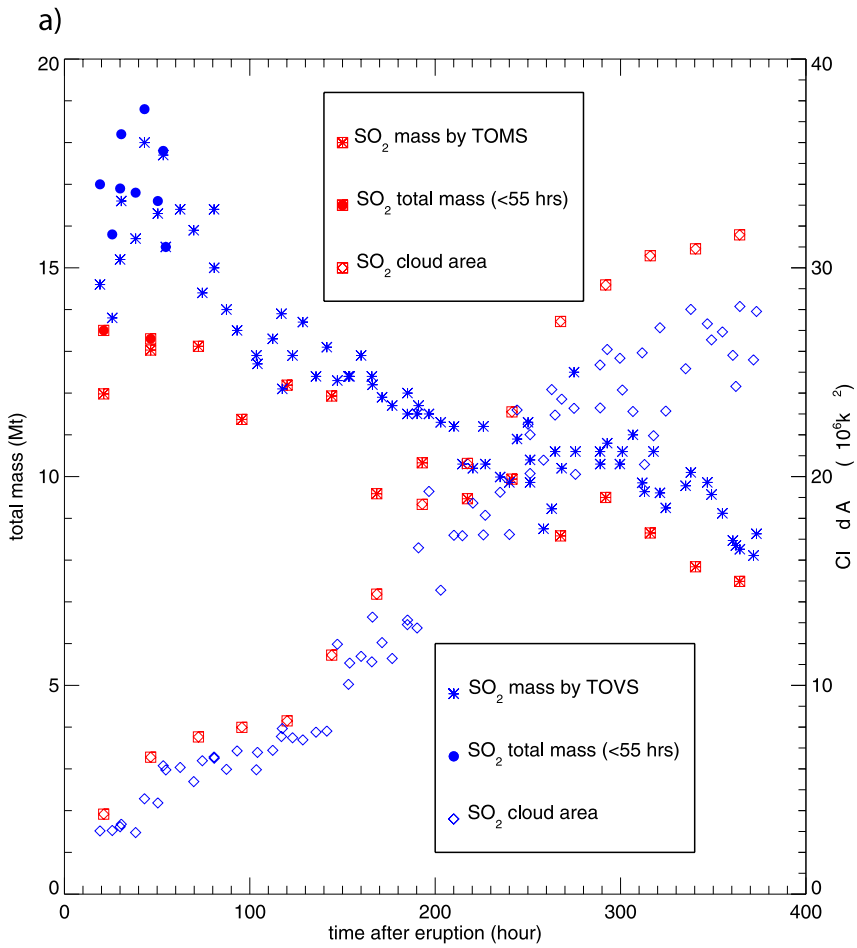

Figure 5. (a) SO_2 mass in Pinatubo cloud and cloud areas as a function of time after eruption, using TOMS and TOVS data (Table 2). SO_2 total masses represented by blue solid dots are the sum of SO_2 mass sensed by TOMS plus SO_2 mass sequestered by ice. (b) Burden of cloud (average mass/area) as a function of time after eruption using TOMS and TOVS data (Table 2).

sulfate (see discussion below) and possibly also partly reflect stratospheric water vapor within the volcanic cloud.

4. Discussion

4.1. Total SO_2 Mass Increase After Eruption

[25] Figure 7 plots the mass of SO_2 in the Pinatubo cloud with time. Early estimates are not plotted (0–19 hrs) because of high cloud density (some cloud areas are invisible to TOVS sensor). No TOMS SO_2 map exists in the first 19 hours after eruption. The increasing trend between 20 and 55–70 hours after eruption is indicated by the TOMS and TOVS data in Figure 6. This increasing trend has also been noted in several other eruptions based on TOMS data (but not TOVS data) [*Bluth et al.*, 1995; *Constantine et al.*, 2000]. In the case of Pinatubo, we would have difficulty demonstrating this result without the higher temporal resolution of TOVS sensing. The average cloud burdens (tonnage/area) from the TOVS (Table 2) also show an increasing trend for ~38 hours after eruption (Figure 5b).

[26] Potential reasons suggested for SO_2 mass increase in other eruptions include: (1) oxidation of co-erupted H_2S to SO_2 [*Bluth et al.*, 1995]; (2) ultraviolet (UV) light scattering by ash which may have partially masked detection of SO_2 [*Bluth et al.*, 1995]; (3) Uncertainty in the mass determinations of SO_2 (10–30%) [*Krueger et al.*, 1995]; and (4) release of gas-phase SO_2 from SO_2 - ice -

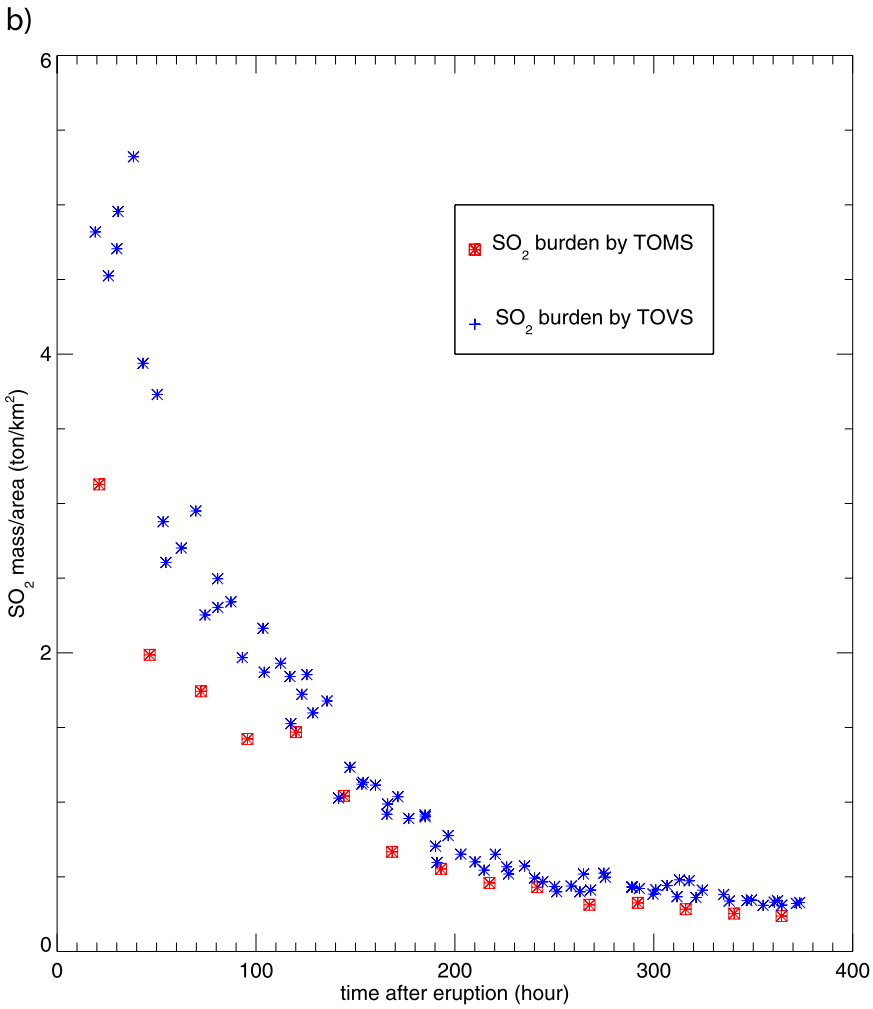

Figure 5. (continued)

Table 2. Summary of TOMS SO_2 Cloud Tonnages and Areas[a]

Date	Time, GMT	Hours After Eruption	SO_2 mass, Mt	Cloud Area ($\times 10^6$ km^2)	SO_2 Burden, ton/km^2	Maximum SO_2, DU
06/16/91	2:01–3:44	21.2	12.0	3.83	3.13	537
06/17/91	2:40–5:45	46.5	13.0	6.56	1.99	423
06/18/91	4:14–7:42	72.3	13.1	7.53	1.74	350
06/19/91	3:02–7:45	95.7	11.4	7.99	1.42	207
06/20/91	3:38–7:57	120.1	12.2	8.30	1.47	180
06/21/91	3:26–8:15	144.2	11.9	11.45	1.04	137
06/22/91	3:44–8:34	168.5	9.6	14.37	0.67	101
06/23/91	4:03–9:22	193.0	10.3	18.67	0.55	78
06/24/91	3:02–11:08	217.4	9.5	20.63	0.46	67
06/25/91	3:45–10:28	241.4	9.9	23.10	0.43	62
06/26/91	4:56–13:40	267.6	8.6	27.43	0.31	59
06/27/91	5:30–13:50	292.0	9.5	29.18	0.33	55
06/28/91	5:31–13:51	316.0	8.7	30.58	0.28	51
06/29/91	5:50–14:25	340.4	7.8	30.91	0.25	45
06/30/91	5:01–14:49	364.2	7.5	31.58	0.24	39

[a] "Hours after eruption" is the time from the start of the eruption to the average of the sensing time in column 2, in hours.

Table 3. Summary of TOVS SO_2 Cloud Tonnages and Area[a]

Date	Time, GMT	Hours After Eruption	SO_2 Mass, Mt	Cloud Area ($\times 10^6$ km^2)	SO_2 Burden, ton/km^2	Maximum SO_2, DU
06/16/91	0:52	19.2	14.6	3.03	4.82	433
	07:28	25.8	13.8	3.05	4.52	441
	11:44	30.1	15.2	3.35	4.54	415
	12:20	30.7	16.6	3.23	5.14	432
	20:05	38.4	15.7	2.95	5.32	456
06/17/91	0:12–1:33	43.2	18.0	4.57	3.94	443
	7:25–8:43	50.4	17.7	6.15	2.88	412
	7:23–14:34	53.3	16.3	4.37	3.73	398
	11:39–13:05	54.7	15.5	5.95	2.61	370
	19:16–20:59	62.4	16.4	6.07	2.70	364
06/18/91	1:55–4:58	69.8	15.9	5.39	2.95	341
	7:25–8:43	74.4	14.4	6.39	2.25	325
	12:41–16:08	80.7	16.4	6.57	2.50	335
	12:53–16:05	80.8	15.0	6.51	2.30	317
	20:47–21:22	87.4	14.0	5.98	2.34	325
06/19/91	1:58–3:41	93.1	13.5	6.86	1.97	236
	12:21–14:05	103.5	12.9	5.96	2.16	223
	12:59–14:40	104.1	12.7	6.79	1.87	222
	21:12–22:54	112.4	13.3	6.89	1.93	205
06/20/91	1:11–4:18	117.1	13.9	7.55	1.84	198
	1:36–4:50	117.5	12.1	7.93	1.52	183
	7:12–10:18	123.1	12.9	7.49	1.72	191
	12:07–15:12	125.6	13.7	7.39	1.85	176
	12:43–15:52	128.6	12.4	7.76	1.60	169
	19:51–22:56	135.7	13.1	7.81	1.68	179
06/21/91	1:42–4:45	141.5	12.3	11.97	1.03	171
	7:45–10:05	147.2	12.4	10.05	1.23	169
	13:21–16:28	153.2	12.4	11.07	1.12	163
	14:01–17:05	153.9	12.9	11.39	1.13	156
	20:08–23:16	160.0	12.4	11.13	1.11	143
06/22/91	1:59–5:01	165.8	12.2	13.27	0.92	135
	2:11–5:30	166.2	11.9	12.05	0.99	128
	7:23–10:38	171.3	11.7	11.29	1.04	124
	12:07–16:51	176.8	11.5	12.91	0.89	111
	21:08–24:13	185.0	12.0	13.13	0.91	91
	21:08–24:23	185.1	11.5	12.75	0.90	105
06/23/91	1:30–6:21	190.2	11.7	16.59	0.71	85
	2:16–7:06	191.0	11.5	19.29	0.60	86
	7:53–12:45	196.6	11.3	14.56	0.78	89
	14:15–19:05	203.0	11.2	17.19	0.65	85
	21:25–2:12	210.1	10.3	17.17	0.60	87
06/24/91	1:58–6:45	214.7	10.2	18.73	0.55	77
	8:25–11:39	220.4	11.2	17.21	0.65	76
	13:15–18:07	226.0	10.3	18.15	0.57	75
	14:18–19:06	227.0	10.0	19.25	0.52	73
	22:19–3:06	235.0	9.9	17.23	0.57	77
06/25/91	3:15–8:11	240.0	10.9	23.19	0.47	79
	8:12–11:29	244.2	11.3	22.51	0.50	80
	13:23–18:12	250.1	10.4	22.01	0.47	82
	14:33–19:12	251.2	9.9	20.15	0.49	76
	21:46–2:31	258.5	8.8	20.79	0.42	80
06/26/91	2:11–6:56	262.9	9.2	24.17	0.38	66
	3:29–9:16	264.7	10.6	22.95	0.46	69
	6:29–13:23	268.3	10.2	23.71	0.43	72
	13:21–19:50	274.9	12.5	23.27	0.53	70
	14:09–20:32	275.7	10.6	20.11	0.52	71

Table 3. (continued)

Date	Time, GMT	Hours After Eruption	SO_2 Mass, Mt	Cloud Area ($\times 10^6$ km^2)	SO_2 Burden, ton/km^2	Maximum SO_2, DU
06/27/91	3:23–9:51	288.9	10.6	25.35	0.41	72
	3:23–9:59	289.0	10.3	23.29	0.44	73
	7:56–13:01	292.8	10.8	26.09	0.41	69
	14:09–20:30	299.6	10.3	25.67	0.40	66
	15:25–21:56	301.0	10.6	24.15	0.44	72
	21:55–2:50	306.7	11.0	23.12	0.48	75
06/28/91	2:13–8:32	311.7	9.9	25.93	0.38	70
	4:07–9:05	312.9	9.6	20.58	0.47	69
	8:15–14:43	317.8	10.6	21.96	0.48	67
	12:23–17:30	321.3	9.6	27.13	0.35	65
	15:36–20:33	324.4	9.3	23.14	0.40	62
06/29/91	2:16–7:20	335.1	9.8	25.17	0.39	57
	4:21–10:50	337.9	10.1	28.01	0.36	60
	13:16–19:45	346.8	9.9	27.32	0.36	57
	15:31–21:59	349.1	9.6	26.55	0.36	59
	22:05–3:12	355.0	9.1	26.93	0.34	60
06/30/91	3:03–9:28	360.6	8.5	25.81	0.33	53
	4:42–11:05	362.2	8.4	24.32	0.34	57
	5:35–14:30	364.4	8.3	28.15	0.29	54
	14:12–20:36	371.7	8.1	25.59	0.31	52
	15:58–22:03	373.3	8.6	27.91	0.31	58

[a] "Hours after eruption" is the time from the start of the eruption to the average of the sensing time in column 2, in hours.

ash mixtures (incorporation, sticking, etc) [*Textor et al.*, 2003].

[27] If the cause of the Pinatubo SO_2 mass increase were mainly due to the oxidation of the co-erupted H_2S to SO_2, then 2–4 Mt H_2S would have to be co-erupted, representing about 10–25% of the total S. *Rutherford and Devine* [1996] calculate that the Pinatubo magma, which includes Fe-Ti oxides, was at 780 ± 10°C just prior to eruption and had an oxygen fugacity of three log units above the nickel-nickel oxygen buffer, or log(fo_2) of −11.5, based on iron-titanium oxide geothermometry for the white pumice from the 1991 Pinatubo eruption. Under these conditions, little H_2S would be produced during eruption. *Gerlach et al.* [1996] indicate that Pinatubo's equilibrium SO_2/H_2S fugacity ratio was >55 during eruption and this oxidized condition precludes significant H_2S contribution. Therefore it is unlikely that 2–4 Mt H_2S could have been co-erupted with 17–20 Mt SO_2 from the Pinatubo eruption.

[28] *Krotkov et al.* [1997] suggest that TOMS SO_2 can be overestimated by 15–25% when significant ash is present in the SO_2 cloud. Guo et al. (submitted manuscript, 2004) concluded that ash fell out very rapidly, so this overestimate would be expected to be strongest on the first day. Overestimation of SO_2 mass for the first day SO_2 mass would thus cause TOMS mass estimates to be higher than the second day, therefore, the presence of ash cannot explain an SO_2 increase 55 hours (2.3 days) after eruption.

[29] It is also unlikely that the second day SO_2 increase was caused by simple uncertainty in retrieval. A 30% uncertainty of TOMS retrieval is a maximum, occurring for large solar zenith angles near swath edges. Under most circumstances the uncertainty is nearer to 10% as stated by *Bluth et al.* [1995]. The accuracy of the retrieved TOVS SO_2 is also estimated to be 5–10% for SO_2 column amounts in the range of 10–800 DU (Prata et al., submitted manuscript, 2004). The SO_2 mass increase trend is independently confirmed by both TOMS (three data points) and TOVS data (9 data points), and it is unlikely uncertainty can explain agreement of two independent methods a and is unlikely to produce a systematic (positive only) bias.

[30] Ice is an important component of many volcanic clouds [*Rose et al.*, 1995; *Mayberry et al.*,

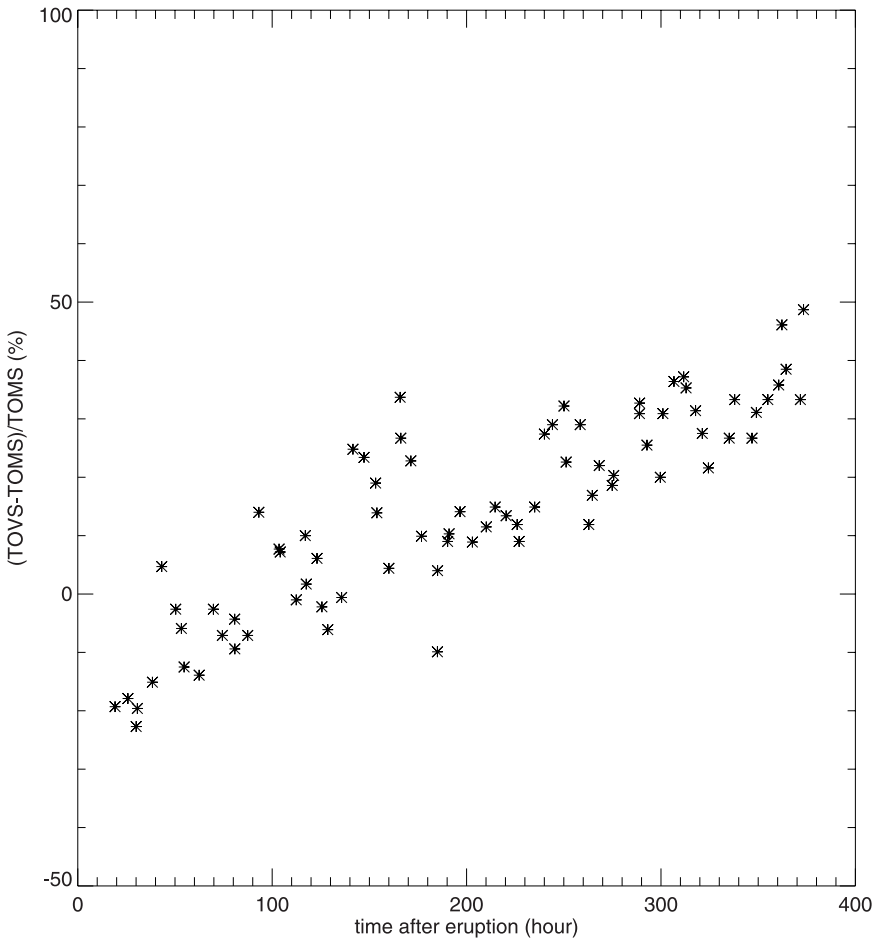

Figure 6. The percent difference of maximum SO_2 pixel values in Dobson Units ((TOVS-TOMS)/TOMS) as a function of time after eruption (data from Tables 2 and 3).

2002; *Rose et al.*, 2003]. *Gerlach et al.* [1996] previously suggests the potential for significant SO_2 adsorption on particle surfaces. *Textor et al.* [2003] have explained how ice can scavenge SO_2 in volcanic clouds. The Pinatubo volcanic cloud entrained H_2O from a very moist tropical atmosphere [*Herzog et al.*, 1998; *Guo et al.*, 2000] and also contained at least 5.1–6.4% of magmatic water vapor [*Rutherford and Devine*, 1996; *Gerlach et al.*, 1996]. The Pinatubo volcanic cloud was subject to co-ignimbrite cloud formation which can further enhance entrainment [*Dartevelle et al.*, 2002]. In addition, there was an active tropical cyclone, Typhoon Yunya, passing the Pinatubo area during the eruption period. Thus significant amounts of water vapor were convected with the volcanic cloud which likely led to significant ice formation. In Pinatubo's case, we speculate that gas scavenging occurring within ice crystals in the stratosphere could release SO_2 again during a period of sublimation or ice/ash aggregation and sedimentation lasting 2–3 days after eruption. The mechanism we envision has several stages: (1) Initial rapid growth of ice on ash nuclei during ascent of the eruption column in which SO_2 is sequestered. (2) Gradual sublimation of ice would be expected after some cloud expansion and drifting through the extremely dry stratosphere, releasing sequestered SO_2. (3) Possibly simultaneously with 2, aggregation of icy ash and fallout within the stratosphere, so that sublimation could release SO_2 at a lower level that some of the other volcanic SO_2. (4) After a few days, most of the ice is gone, sublimated completely or possibly partly fallen out of the stratosphere completely. Ice mass decreases in a stratospheric volcanic ice cloud were described by *Rose et al.* [2003] in the case of the 2000 eruption of Hekla, Iceland. A maximum

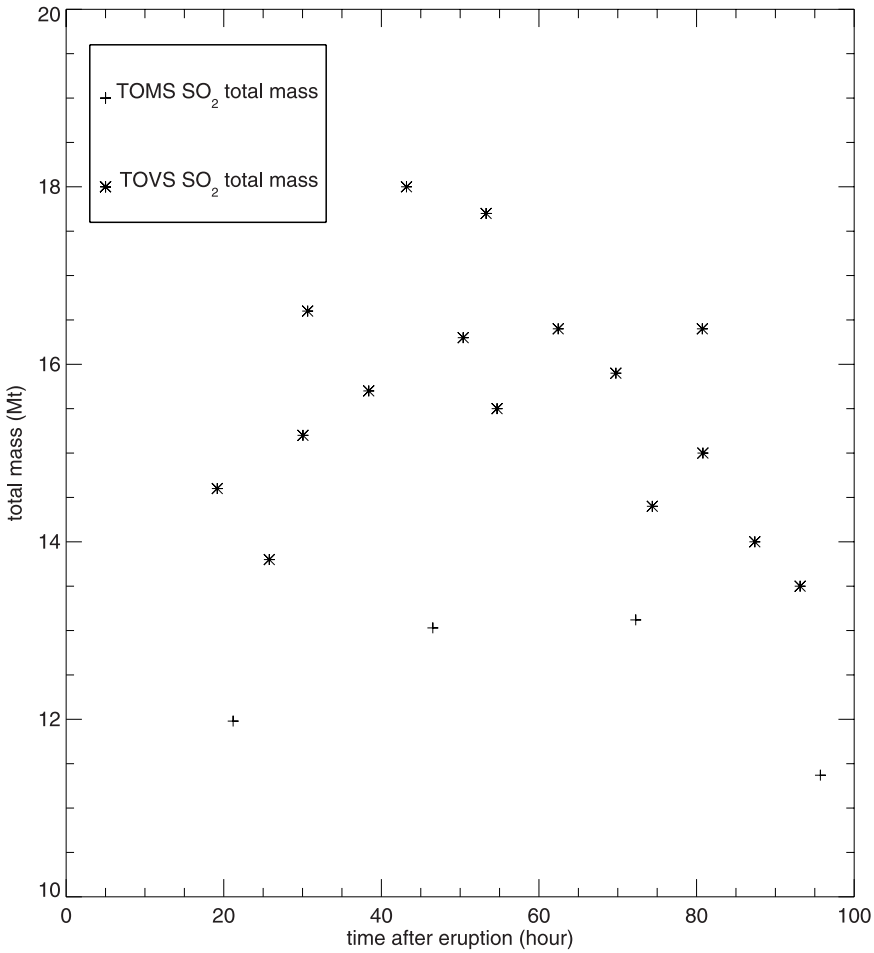

Figure 7. SO_2 mass estimates (Tables 1 and 2) with time for the first 100 hours after eruption. Both TOMS and TOVS data show increase in SO_2 mass after eruption during the period from 20 to about 50 hours.

mass of ~80 Mt of ice or ice-ash mixtures in the range of 1–30 μm in the Pinatubo ash cloud is suggested from AVHRR and HIRS/2 data [*Guo et al.*, 2004]. Therefore SO_2 could be incorporated with ice-ash mixtures as inclusions [*Textor et al.*, 2003] or adsorbed on the surface of ice-ash mixtures. Later SO_2 is released from these mixtures when ice sublimates in the dry stratosphere or alternatively, ice-ash aggregation and sedimentation processes can also cause gas-phase SO_2 release from the gas-ash-ice mixture [*Textor*, 1999]. Only a second day SO_2 mass increase was found for other eruptions [*Bluth et al.*, 1995]. The most reasonable cause for the longer duration of SO_2 mass increase (55–70 hours after eruption) in the 1991 Pinatubo erupted volcanic clouds could be that more ice exists in the Pinatubo volcanic clouds than any other smaller eruptions. The existence of the large amount of ice in the clouds requires a longer time to release gas phase SO_2 from the ash-ice mixture.

[31] In summary, the SO_2 mass increase within the Pinatubo clouds after the start of the eruption is most probably caused by the gas-phase SO_2 release from the ice-ash-gas mixtures. The released gas-phase SO_2 is estimated at about 1 and 3 Mt by TOMS and TOVS data, respectively (Figure 6), using the best fit exponential curve for the data during the period of 20–55 hours after eruption. The use of exponential curve is based on the mechanism of gas release from ice used in the numerical model ATHAM [*Diehl et al.*, 1998; *Textor*, 1999].

[32] Another interesting observation from the imagery (Figure 3) shows the trailing portion of the Pinatubo cloud drifting at a vastly slower rate than

the leading edge. In fact, by June 30, the trailing edge has only drifted as far as western Indonesia (about 3000 km). This could result from the vertical distribution of the erupted sulfur dioxide mass and a vertical (regional) wind gradient, or an effect of subliming ice releasing SO_2 over a period of days. The "tail-end" cloud dynamics from large eruptions could well be a focus for future studies, as they can produce unexpected, but persistent impacts on regional aviation.

[33] The process of ice sequestration as suggested in this paper is of potential importance in other tropical eruptions as well. The mass of H_2O which is carried to the stratosphere is controlled by inputs of magmatic H_2O, entrainment of atmospheric moisture, and by processes that occur as the volcanic plume rises to the stratosphere. It is possible that there could be contributions of water from near surface as well (ocean water, lakes, glaciers, hydrothermal systems), depending on the environment of the volcano. The 1994 eruption of Rabaul had substantial seawater contribution, which explains in part the large ice content of the stratospheric cloud that resulted [*Rose et al.*, 1994]. The 26 December 1997 eruption at Montserrat also caused a large transfer of oceanic water to the upper troposphere and stratosphere [*Mayberry et al.*, 2002].

[34] At Pinatubo, seawater was not a major contributor as the ocean is far (35 km) from the active vent. The minimum mass of water vapor released as part of the magmatic eruption was estimated at 95 Mt by *Gerlach et al.* [1996]. In the tropical atmosphere, the masses of water vapor in the lower (0–3 km) troposphere is much higher than at high latitudes, so entrainment of air could result in an order of magnitude or more entrained water in the eruption column than would be found in high latitude eruptions [*Textor et al.*, 2003]. The amounts of entrained water vapor could be even more enhanced in co-ignimbrite clouds such as those that occurred at Pinatubo [*Dartevelle et al.*, 2002]. During convective vertical transport in the eruption column, water vapor will have phase changes which influence dynamics and which could result in substantial H_2O loss [*Herzog et al.*, 1998]. Although these issues represent undefined and underinvestigated uncertainties, we suggest that many tropical eruptions have substantial similarity to Pinatubo, especially with respect to high ambient lower tropospheric moisture that could be entrained. It is likely that most tropical eruptions that reach the stratosphere could carry enough H_2O in the form of ice that sequestration of SO_2 could occur in an analogous way. Therefore the SO_2 mass increases after eruption detected in other eruptions using remote sensing could at least be partially explained by the abundance of stratospheric ice.

4.2. Estimate of the Initially Released SO_2 Mass and Its e-Folding Time

[35] The initial mass of SO_2 and its conversion/removal rate can be estimated by using best fit exponential curves assuming first order chemical reaction rates [*McKeen et al.*, 1984; *Krueger et al.*, 1995]. Decay of SO_2 masses in the Pinatubo clouds show curved trends (Figure 5a). The total SO_2 (filled circles) masses include SO_2 that was sequestered by ice in the early Pinatubo cloud (Figure 5a). The sequestered SO_2 masses were calculated assuming an exponential release of SO_2 from ice [*Diehl et al.*, 1998; *Textor*, 1999].

[36] Analysis of e-folding times using different time periods (Table 4) indicates that the SO_2 removal rate was much faster in the first 118 hours after eruption (20 days for TOMS and 12 days for TOVS), then slows to a relatively constant rate after 118 hours (25 days e-folding for both TOMS and TOVS). We assert that the change in rate is caused by the decreasing catalysis of ice and ash with time. Early on, the cloud contains a high surface area from numerous ice and ash particles but this is quickly reduced by both sublimation and fallout. 99% of ash and ice were removed from atmosphere 112 hours after eruption [*Guo et al.*, 2004]. It is known that the volcanic SO_2 will be oxidized to sulfate aerosol in the atmosphere [*Turco et al.*, 1983; *Tabazadeh and Turco*, 1993]. The conversion rate of SO_2 may vary with environmental conditions, such as the amount of ash or sulfate aerosol within the volcanic SO_2 cloud, the intensity of solar radiation, the temperature of the cloud, and the amount of ice and ash within the volcanic cloud.

Table 4. SO_2 Initial Masses and Its e-Folding Times With Different Time Period Data Used[a]

Satellite Sensor	Time Period Used (Hours After Eruption)	Exponential Fitting Curve	e-Folding Time, days
TOMS	19–118	$Y = 14.5e^{-0.0021x}$	20
TOMS	118–374	$Y = 14.5e^{-0.0017x}$	25
TOMS	19–374	$Y = 14.2e^{-0.0017x}$	25
TOVS	19–118	$Y = 19.4e^{-0.0034x}$	12
TOVS	118–170	$Y = 16.1e^{-0.0017x}$	25
TOVS	170–251	$Y = 15.8e^{-0.0017x}$	25
TOVS	251–374	$Y = 15.9e^{-0.0017x}$	25
TOVS	19–374	$Y = 17.0e^{-0.002x}$	23

[a] SO_2 sequestered by ice in the early cloud stage are included in total SO_2 masses in TOVS fittings because sulfate produces a positive interference.

[37] Considering the potential oxidants (OH and O_3) in the atmosphere, the factors that might influence the SO_2 oxidation rate are even more complicated. For example, the sublimation of ice in the stratospheric volcanic cloud due to the extremely low relative humidity in the stratosphere will increase the gas phase H_2O. Photolysis of H_2O in the stratosphere (high UV intensity) will increase the OH concentration in the stratosphere, which will result in a higher oxidation rate for SO_2 in the stratospheric volcanic cloud. The increase of OH concentration in the stratosphere after larger volcanic eruptions has been reported by *McKeen et al.* [1984]. They observed that the column OH concentrations increased 30% above the previous 5 years following the 1992 El Chichón eruption. For Pinatubo case, more SO_2 might be oxidized in the first 4–5 days after eruption, during the period when ice sublimation was also occurring.

[38] We use data from clouds which have been in the atmosphere between 19 and 118 hours after eruption onset (the total SO_2 masses include SO_2 masses sequestered by ice in the early cloud) to estimate initially released SO_2 mass. Data within this fast SO_2 conversion period can provide a more accurate estimation of initially released SO_2 mass. Data <19 hours are excluded because of the existence of unmapped cloud areas due to the cloud opacity. The equation of the best fit exponential curve for TOMS data is $y = 14.5e^{-0.0021}$. Considering the maximum uncertainty of 10% for TOMS SO_2 retrieval, uncertainty of 2% for TOMS SO_2 image reconstruction, 3% uncertainty for cloud height estimation, and uncertainty of 15% for exponential curve fitting, the total uncertainty for TOMS method is estimated to be 20%. The initial cloud mass of SO_2 is thus 15 ± 3 Mt. Using TOVS data for the same time period, the equation of the best fitting exponential curve is $y = 19.4e^{-0.0034}$. Considering the maximum uncertainty of 10% for TOVS SO_2 retrieval, uncertainty of 10% for TOVS SO_2 image reconstruction, 3% uncertainty for cloud height estimation, and uncertainty of 14% for exponential curve fitting, the total uncertainty for TOVS method is estimated to be 20%. Therefore the TOVS initial cloud mass of SO_2 is estimated at 19 ± 4 Mt. If a best fit linear curve (which represents a zero order oxidation process) is used, identical masses are estimated using linear and exponential best fittings for both TOMS and TOVS data (15 Mt and 19 Mt, respectively). The data within the whole time period are used to estimate the e-folding time as they can provide a more accurate estimation of the overall e-folding time with the changing removal rate. In this way, the best fit exponential curves are $y = 14.2e^{-0.0017}$ and $y = 17.0e^{-0.0018}$ for TOMS and TOVS, respectively. The e-folding times are thus 25 ± 5 days for TOMS and 23 ± 5 days for TOVS. These calculations assume a single exponential rate occurs throughout the removal process. However, it appears that the rate is even faster during the first few days when ice and ash are abundant and are catalyzing removal reactions (see above).

[39] These estimates of initial SO_2 based on extrapolation of time based decay trends do not include another part of the "initial SO_2" in the Pinatubo eruption: SO_2 which was apparently rapidly catalyzed to sulfate aerosol during or very shortly after eruption.

Table 5. Summary of Results From This Paper and Previous Work

	This Paper		Previous Work		
Sensor	TOMS	TOVS	TOMS[a]	SBUV[b]	MLS[c]
Initial SO_2 mass (Mt)	18 ± 4[d]	19 ± 4[d]	20 ± 6	12–15	17[c]
SO_2 e-folding time (days)	25 ± 5	23 ± 5	35 ± 11	24 ± 5	33[c]

[a] *Bluth et al.* [1992].
[b] *McPeters* [1993].
[c] *Reed et al.* [1993], uncertainty unknown.
[d] Initially released SO_2 mass includes SO_2 sequestered in ice and SO_2 converted to sulfate during the rise of volcanic plume.

[40] Sulfate aerosol masses in the earliest Pinatubo volcanic cloud were estimated at 4 Mt by multispectral IR retrievals [*Guo et al.*, 2004]. This sulfate would be equivalent to about 3 Mt SO_2 if we assume all such sulfate (75% SO_4^{2-} + 25% H_2O) came from erupted SO_2. The sulfate has absorption in IR similar to SO_2 so it will produce an enhanced SO_2 result, but nothing like this happens in the UV range. Therefore the effects of sulfate in the volcanic cloud are reflected in retrieved TOVS SO_2 mass, but not in retrieved TOMS SO_2 mass. Thus the total initial SO_2 mass is 18 ± 4 Mt (15 SO_2 + 3 SO_2 as sulfate) Mt for TOMS, and 19 ± 4 Mt for TOVS. Table 5 compares these estimates with previously published ones.

[41] The variation of the SO_2 oxidation rate with time (Table 4) is consistent with a catalytic effect of abundant volcanic ash/ice mixtures in young (1–2 day old) volcanic clouds. In the case of Pinatubo the source of the ice in the volcanic cloud is both magmatic H_2O and entrained lower tropospheric air which is very moist in the tropics. It is likely that the same conditions exist in most tropical volcanic clouds, and thus they too should contain abundant ice as well as ash in their first days of atmospheric residence. Thus SO_2 conversion rates could be accelerated similarly for a few days after most tropical eruptions, until the stratospheric ice sublimes. Laboratory experiments or tests to study the catalytic effects more quantitatively might be of interest.

4.3. Why do TOMS and TOVS Retrievals Differ?

[42] Although data from both sensors display the same trends in SO_2 sequestration to ice, and removal patterns, the TOVS retrievals are consistently higher than TOMS. Figure 6 shows an increasing trend of maximum pixel value from TOVS compared to TOMS. The reason could be due to the gradual increase of sulfate mass due to continuous oxidation of SO_2 within the whole volcanic cloud. This is because sulfate aerosol will absorb at 7.34 μm and not in the UV wavelengths used for the TOMS retrievals. No correction for sulfate absorption is used in the TOVS retrieval model. Gradual sulfate mass increase over time after eruption was found in multispectral IR retrievals, consistent with the decrease of SO_2 mass within the Pinatubo volcanic cloud [*Guo et al.*, 2004]. Therefore SO_2 must be overestimated by the TOVS sensor by an increasing factor as the cloud ages. This effect is partially counteracted by the smaller cloud area detected by TOVS (Tables 2 and 3).

[43] The difference between TOMS and TOVS retrievals suggest the importance of sulfate absorption in the IR range to TOVS (IR) retrieval. Therefore the effects of sulfate absorption need to be considered in IR retrievals. Although the trend is in the right direction and the magnitude is approximately right, the differences between TOMS and TOVS retrievals might not be only due to sulfate interference. Other factors, such as water vapor within and perhaps below the volcanic cloud, need also to be investigated.

5. Conclusions

[44] In this study we analyzed 77 TOVS (infrared) images and re-analyzed 16 TOMS (ultraviolet) images of the Pinatubo SO_2 cloud during its first 15 days of atmospheric residence. Similar SO_2 cloud maps were delineated by TOMS and TOVS

sensors during this period. TOVS SO_2 mass estimates are typically higher than TOMS SO_2 mass estimates by 5–30%. This is most noticable when comparing individual pixel retrievals. The percent difference between TOVS and TOMS maximum pixel values increases with time, and thus the TOVS maximum pixel values are up to 40–50% higher than TOMS maximum pixel values 370 hours after eruption. We suspect that these differences are at least partly caused by sulfate aerosols in the SO_2 cloud, which elevate TOVS SO_2 burdens, but not the TOMS. This effect is not as noticable in overall cloud masses, because the SO_2 cloud areas using TOVS data are smaller than those using TOMS data, especially one week after eruption. The smaller TOVS areas are probably caused by water vapor (below the SO_2 cloud) interference in TOVS which is more severe when SO_2 cloud is thin.

[45] Together with other data, our SO_2 remote sensing results allow us to visualize the distribution of species in the Pinatubo cloud (Figure 1). TOMS and TOVS results show an increase in SO_2 mass after the start of the eruption for about two days, which we speculate may be caused by ice, which initially forms within the stratospheric umbrella cloud and captures some SO_2. The increase in SO_2 results from release by ice during sublimation and transport in the stratospheric volcanic cloud during the first two days of residence. Mass estimates of initially released SO_2 based on extrapolation of remote sensing SO_2 volcanic cloud data are 15 ± 3 Mt for TOMS and 19 ± 4 Mt for TOVS. To estimate the total S released in the eruption SO_2 which was rapidly converted to sulfate aerosol during eruption must also be included. This sulfate mass, estimated at about 3 Mt, causes a proportional overestimate in retrieved TOVS SO_2, but not in TOMS SO_2 mass. Thus the total S release by Pinatubo, calculated as SO_2, is 18 ± 4 Mt based on TOMS and 19 ± 4 Mt based on TOVS. Thus the results from the two detectors agree within expected error ranges when the effects of sulfate interference are considered. After 55 hours residence, SO_2 decreases in the volcanic cloud describe overall e-folding times of 25 ± 5 days for TOMS and 23 ± 5 days for TOVS. The data from both detectors show faster SO_2 removal rates during the first 118 hours of stratospheric residence, an effect that is consistent with catalytic effects of ice and ash which is abundant in the early volcanic cloud, but which falls out quickly. SO_2 mass increases in the volcanic cloud during the first two days after eruption is most probably caused by the gas-phase SO_2 release from the ice-ash-gas mixtures. This result indicates ice-sequestered SO_2 probably exists in all tropical volcanic clouds, and could at least partially explain SO_2 mass increases after eruption observed in many other eruptions.

Acknowledgments

[46] Support for this work came from the National Science Foundation (NSF EAR01-06875) and the National Aeronautics and Space Administration (NAG5-11062), and Song Guo was supported by a NASA Graduate Student Fellowship. We also benefited from comments by Arlin Krueger and an anonymous reviewer.

References

Avdyushin, S. I., G. F. Tulinov, M. S. Ivanov, B. N. Kuzmenko, I. R. Mezhuev, B. Nardi, A. Hauchecorne, and M. L. Chanin (1993), Spatial and temporal evolution of the optical thickness of the Pinatubo aerosol cloud in the northern hemisphere from a network of ship-borne and stationary lidars, *Geophys. Res. Lett.*, *20*, 1963–1966.

Bekki, S., and J. A. Pyle (1994), A two-dimensional modeling study of the volcanic eruption of Mount Pinatubo, *J. Geophys. Res.*, *99*, 18,861–18,869.

Bluth, G. J. S., S. D. Doiron, C. C. Schnetzler, A. J. Krueger, and L. S. Walter (1992), Global tracking of the SO_2 clouds from the June 1991 Mount Pinatubo eruptions, *Geophys. Res. Lett.*, *19*, 151–154.

Bluth, G. J. S., C. C. Schnetzler, A. J. Krueger, and L. S. Walter (1993), The contribution of explosive volcanism to global atmospheric sulfur dioxide concentrations, *Nature*, *366*, 327–329.

Bluth, G. J. S., T. J. Casadevall, C. C. Schnetzler, S. D. Doiron, L. S. Walter, A. J. Krueger, and M. Badruddin (1994), Evaluation of sulfur dioxide emissions from explosive volcanism: The 1982–1983 eruptions of Galunggung, Java, Indonesia, *J. Volcanol. Geotherm. Res.*, *63*, 243–256.

Bluth, G. J. S., C. J. Scott, I. E. Sprod, C. C. Schnetzler, A. J. Krueger, and L. S. Walter (1995), Explosive emissions of sulfur dioxide from the 1992 Crater Peak eruptions, Mount Spurr Volcano, Alaska, *U.S. Geol. Surv. Bull.*, *2139*, 37–46.

Bluth, G. J. S., W. I. Rose, I. E. Sprod, and A. J. Krueger (1997), Stratospheric loading from explosive volcanic eruptions, *J. Geol.*, *105*, 671–683.

Carn, S. A., A. J. Krueger, G. J. S. Bluth, S. J. Schaefer, N. A. Krotkov, I. M. Watson, and S. Datta (2003), Volcanic eruption detection by the Total Ozone Mapping Spectrometer (TOMS) instruments: A 22-year record of sulphur dioxide and ash emissions, in *Volcanic Degassing*, edited by C. Oppenheimer, D. M. Pyle, and J. Barclay, *Geol. Soc. Spec. Publ.*, 213, 177–202.

Constantine, E. K., G. J. S. Bluth, and W. I. Rose (2000), TOMS and AVHRR sensors applied to drifting volcanic clouds from the August 1991 eruptions of Cerro Hudson, in *Remote Sensing of Active Volcanism*, *Geophys. Monogr. Ser.*, vol. 116, edited by P. J. Mouginis-Mark, J. A. Crisp, and J. H. Fink, pp. 45–64, AGU, Washington, D. C.

Dartevelle, S., G. G. J. Ernst, J. Stix, and A. Bernard (2002), Origin of the Mount Pinatubo climactic eruption cloud: Implication for volcanic hazards and atmospheric impacts, *Geology*, *30*, 663–666.

DeFoor, T. E., E. Robinson, and S. Ryan (1992), Early lidar observations of the June 1991 Pinatubo eruption plume at Mauna Loa Observatory, Hawaii, *Geophys. Res. Lett.*, *19*, 187–190.

Deshler, T., D. J. Hofmann, B. J. Johnson, and W. R. Rozier (1992), Balloonborne measurements of the Pinatubo aerosol size distribution and volatility at Laramie, Wyoming during the summer of 1991, *Geophys. Res. Lett.*, *19*, 199–202.

Diehl, K., S. K. Mitra, and H. R. Pruppacher (1998), A laboratory study on the uptake of HCl, HNO_3, and SO_2 gas by ice crystals and the effect of these gases on the evaporation rate of the crystals, *Atmos. Res.*, *47*/*48*, 235–244.

Gerlach, T. M., H. R. Westrich, and R. B. Symonds (1996), Preeruption Vapor in Magma of the Climactic Mount Pinatubo Eruption: Source of the Giant Stratospheric Sulfur Dioxide Cloud, in *Fire and Mud: Eruptions and Lahars of Mount Pinatubo, Philippines*, edited by C. G. Newhall and R. S. Punongbayan, pp. 415–433, Univ. of Wash. Press, Seattle.

Guo, S., W. I. Rose, G. J. S. Bluth, and I. M. Watson (2004), Particles in the great Pinatubo volcanic cloud of late June 1991: The role of ice, *Geochem. Geophys. Geosyst.*, doi:10.1029/2003GC000655, in press.

Guo, S., W. I. Rose, G. J. S. Bluth, C. Textor, and H.-F. Graf (2000), ATHAM model simulation of 15 June 1991 Pinatubo Volcanic plume, *Eos Trans. AGU*, *81*(48), Fall Meet. Suppl., Abstract V62C-10.

Herzog, M., H.-F. Graf, C. Textor, and J. M. Oberhuber (1998), The effect of phase changes of water on the development of volcanic plumes, *J. Volcanol. Geotherm. Res.*, *87*, 55–74.

Holasek, R. E., S. Self, and A. W. Woods (1996), Satellite observations and interpretation of the 1991 Mount Pinatubo eruption plumes, *J. Geophys. Res.*, *101*, 27,635–27,655.

Jaeger, H. (1992), The Pinatubo eruption cloud observed by lidar at Garmisch-Partenkirchen, *Geophys. Res. Lett.*, *19*, 191–194.

Kidwell, K. B. (Ed.) (1998), NOAA-Polar Orbiter Data User's Guide, Natl. Environ. Satellite, Data, and Info. Serv., Silver Spring, Md.

Kinne, S., O. B. Toon, and M. J. Prather (1992), Buffering of stratospheric circulation by changing amounts of tropical ozone: A Pinatubo case study, *Geophys. Res. Lett.*, *19*, 1927–1930.

Krotkov, N. A., A. J. Krueger, and P. K. Bhartia (1997), Ultraviolet optical model of volcanic clouds for remote sensing of ash and sulfur dioxide, *J. Geophys. Res.*, *102*, 21,891–21,904.

Krotkov, N. A., O. Torres, C. Seftor, A. J. Krueger, W. Rose, A. Kostinski, G. Bluth, D. Schneider, and S. J. Schaefer (1999), Comparison of TOMS and AVHRR volcanic ash retrievals from the August 1992 eruption of Mt. Spurr, *Geophys. Res. Lett.*, *26*, 455–458.

Krueger, A. J. (1983), Sighting of El Chichon sulfur dioxide clouds with the Nimbus 7 Total Ozone Mapping Spectrometer, *Science*, *220*, 1377–1379.

Krueger, A. J., L. S. Walter, P. K. Bhartia, C. C. Schnetzler, N. A. Krotkov, I. Sprod, and G. J. S. Bluth (1995), Volcanic sulfur dioxide measurements from the Total Ozone Mapping Spectrometer (TOMS) instruments, *J. Geophys. Res.*, *100*, 14,057–14,076.

Krueger, A. J., S. J. Schaefer, N. A. Krotkov, G. J. S. Bluth, and S. Barker (2000), Ultraviolet remote sensing of volcanic emissions, in *Remote Sensing of Active Volcanism*, *Geophys. Monogr. Ser.*, vol. 116, edited by P. J. Mouginis-Mark, J. A. Crisp, and J. H. Fink, pp. 25–43, AGU, Washington, D. C.

Liu, X., and J. E. Penner (2002), Effect of Mount Pinatubo H_2SO_4/H_2O aerosol on ice nucleation in the upper troposphere using a global chemistry and transport model, *J. Geophys. Res.*, *107*(D12), 4141, doi:10.1029/2001JD000455.

Mayberry, G. C., W. I. Rose, and G. J. S. Bluth (2002), Dynamics of volcanic and meteorological clouds produced on 26 December (Boxing Day) 1997 at Soufriere Hills Volcano, Montserrat, in *The eruption of Soufriere Hills Volcano, Montserrat, from 1995 to 1999*, edited by T. H. Druitt and B. P. Kokelaar, *Mem. Geol. Soc. London*, *21*, 539–555.

McCormick, A. P., L. W. Thomason, and C. R. Trepte (1995), Atmospheric effects of Mt. Pinatubo eruptions, *Nature*, *373*, 399–404.

McKeen, S. A., S. C. Liu, and C. S. Kiang (1984), On the chemistry of stratospheric SO_2 from volcanic eruptions, *J. Geophys. Res.*, *89*, 4873–4881.

McPeters, R. D. (1993), The atmospheric SO2 budget for Pinatubo derived from NOAA-11 SBUV/2 spectral data, *Geophys. Res. Lett.*, *20*, 1971–1974.

McPeters, R. D., et al. (1996), *Nimbus-7 Total Ozone Mapping Spectrometer* (*TOMS*) *Data Product User's Guide*, NASA, Washington, D. C.

Pierluissi, J. H., and K. Tomiyama (1980), Numerical methods for the generation of empirical and analytical transmittance functions with applications to trace gases, *App. Optics*, *19*, 2298–2309.

Reed, W. G., L. Froidevaux, and J. W. Waters (1993), Microwave limb sounder measurement of stratospheric SO_2 from the Mt. Pinatubo volcano, *Geophys. Res. Lett.*, *20*, 1299–1302.

Robock, A. (2002), The Climate Aftermath, *Science*, *295*, 1242–1243.

Rose, W. I., D. J. Delene, D. J. Schneider, G. J. S. Bluth, A. J. Krueger, I. Sprod, C. McKee, H. L. Davies, and G. G. J.

Ernst (1995), Ice in the 1994 Rabaul eruption cloud: Implications for volcano hazard and atmospheric effects, *Nature*, *375*, 477–479.

Rose, W. I., et al. (2003), The February–March 2000 eruption of Hekla, Iceland from a satellite perspective, in Volcanism and the Earth's Atmosphere, *Geophys. Monogr. Ser.*, vol. 139, edited by A. Robock and C. Oppenheimer, pp. 107–132, AGU, Washington, D. C.

Rutherford, M. J., and J. D. Devine (1996), Preeruption Pressure-Temperature Conditions and Volatiles in the 1991 Dacitic Magma of Mount Pinatubo, in *Fire and Mud: Eruptions and Lahars of Mount Pinatubo, Philippines*, edited by C. G. Newhall and R. S. Punongbayan, pp. 751–766, Univ. of Wash. Press, Seattle.

Schnetzler, C. C., A. J. Krueger, G. S. Bluth, I. E. Sprod, and L. S. Walter (1995), Comment on "The atmospheric SO_2 budget for Pinatubo derived from NOAA-11 SBUV/2 spectral data" by R. D. McPeters, *Geophys. Res. Lett.*, *22*, 315–316.

Seftor, C. J., N. C. Hsu, J. R. Herman, P. K. Bhartia, O. Torres, W. I. Rose, D. J. Schneider, and N. Krotkov (1997), Detection of volcanic ash clouds from Nimbus 7/total ozone mapping spectrometer, *J. Geophys. Res.*, *102*, 16,749–16,759.

Solomon, S., R. W. Sanders, R. R. Garcia, and J. G. Keys (1993), Increased chlorine dioxide over Antarctica caused by volcanic aerosols from Mount Pinatubo, *Nature*, *363*, 245–248.

Tabazadeh, A., and R. P. Turco (1993), Stratospheric chlorine injection by volcanic eruptions: HCl scavenging and implications for ozone, *Science*, *260*, 1082–1086.

Textor, C. (1999), Numerical Simulation of Scavenging Processes in Explosive Volcanic Eruption Clouds, Ph.D. thesis, Max-Planck Inst. for Meteorol., Hamburg, Germany.

Textor, C., H.-F. Graf, M. Herzorg, and J. M. Oberhuber (2003), Injection of gases into the stratosphere by explosive volcanic eruptions, *J. Geophys. Res.*, *108*, 4606–4623.

Timmreck, C., H.-F. Graf, and J. Feichter (1999), Simulation of Mt. Pinatubo Volcanic aerosol with the Hamburg Climate Model ECMAM4, *Theor. Appl. Climatol.*, *62*, 85–108.

Turco, R. P., O. B. Toon, R. C. Whitten, P. Hamill, and R. G. Keesee (1983), The 1980 eruptions of Mount St. Helens: Physical and chemical processes in the stratospheric clouds, *J. Geophys. Res.*, *88*, 5299–5319.

Wallace, P., S. Carn, W. I. Rose, T. Gerlach, and G. J. S. Bluth (2003), Integrating petrologic and remote sensing perspectives on magmatic volatiles and volcanic degassing, *Eos Trans. AGU*, *84*(42), 441–447.

Wolfe, E. W., and R. P. Hoblitt (1996), Overview of the Eruptions, in *Fire and Mud: Eruptions and Lahars of Mount Pinatubo, Philippines*, edited by C. G. Newhall and R. S. Punongbayan, pp. 415–433, Univ. of Wash. Press, Seattle.

Yu, T., and W. I. Rose (2000), Retrieval of sulfate and silicate ash masses in Young (1 to 4 days) eruption clouds using multiband infrared HIRS/2 data, in *Remote Sensing of Active Volcanism*, *Geophys. Monogr. Ser.*, vol. 116, edited by P. J. Mouginis-Mark, J. A. Crisp, and J. H. Fink, pp. 87–100, AGU, Washington, D. C.